Am J Physiol Gastrointest Liver Physiol 312: G374–G389, 2017.
First published February 2, 2017; doi:10.1152/ajpgi.00386.2016.

RESEARCH ARTICLE | *Neurogastroenterology and Motility*

Nitric oxide regulates homeoprotein OTX1 and OTX2 expression in the rat myenteric plexus after intestinal ischemia-reperfusion injury

Viviana Filpa,[1]* Elisa Carpanese,[1]* Silvia Marchet,[1] Cristina Pirrone,[1] Andrea Conti,[1] Alessia Rainero,[1] Elisabetta Moro,[2] Anna Maria Chiaravalli,[3] Ileana Zucchi,[4] Andrea Moriondo,[1] Daniela Negrini,[1] Francesca Crema,[2] Gianmario Frigo,[2] Cristina Giaroni,[1] and Giovanni Porta[1]

[1]*Department of Medicine and Surgery, University of Insubria, Varese, Italy;* [2]*Department of Internal Medicine and Therapeutics, Section of Pharmacology, University of Pavia, Pavia, Italy;* [3]*Department of Pathology, Ospedale di Circolo, Varese, Italy; and* [4]*ITB Consiglio Nazionale delle Ricerche, Segrate, Milan, Italy*

Submitted 28 October 2016; accepted in final form 27 January 2017

Filpa V, Carpanese E, Marchet S, Pirrone C, Conti A, Rainero A, Moro E, Chiaravalli AM, Zucchi I, Moriondo A, Negrini D, Crema F, Frigo G, Giaroni C, Porta G. Nitric oxide regulates homeoprotein OTX1 and OTX2 expression in the rat myenteric plexus after intestinal ischemia-reperfusion injury. *Am J Physiol Gastrointest Liver Physiol* 312: G374–G389, 2017. First published February 2, 2017; doi:10.1152/ajpgi.00386.2016.—Neuronal and inducible nitric oxide synthase (nNOS and iNOS) play a protective and damaging role, respectively, on the intestinal neuromuscular function after ischemia-reperfusion (I/R) injury. To uncover the molecular pathways underlying this dichotomy we investigated their possible correlation with the orthodenticle homeobox proteins OTX1 and OTX2 in the rat small intestine myenteric plexus after in vivo I/R. Homeobox genes are fundamental for the regulation of the gut wall homeostasis both during development and in pathological conditions (inflammation, cancer). I/R injury was induced by temporary clamping the superior mesenteric artery under anesthesia, followed by 24 and 48 h of reperfusion. At 48 h after I/R intestinal transit decreased and was further reduced by N^{ω}-propyl-L-arginine hydrochloride (NPLA), a nNOS-selective inhibitor. By contrast this parameter was restored to control values by 1400W, an iNOS-selective inhibitor. In longitudinal muscle myenteric plexus (LMMP) preparations, iNOS, OTX1, and OTX2 mRNA and protein levels increased at 24 and 48 h after I/R. At both time periods, the number of iNOS- and OTX-immunopositive myenteric neurons increased. nNOS mRNA, protein levels, and neurons were unchanged. In LMMPs, OTX1 and OTX2 mRNA and protein upregulation was reduced by 1400W and NPLA, respectively. In myenteric ganglia, OTX1 and OTX2 staining was superimposed with that of iNOS and nNOS, respectively. Thus in myenteric ganglia iNOS- and nNOS-derived NO may promote OTX1 and OTX2 upregulation, respectively. We hypothesize that the neurodamaging and neuroprotective roles of iNOS and nNOS during I/R injury in the gut may involve corresponding activation of molecular pathways downstream of OTX1 and OTX2.

NEW & NOTEWORTHY Intestinal ischemia-reperfusion (I/R) injury induces relevant alterations in myenteric neurons leading to dismotility. Nitrergic neurons seem to be selectively involved. In the present study the inference that both neuronal and inducible nitric oxide synthase (nNOS and iNOS) expressing myenteric neurons may undergo important changes sustaining derangements of motor function is reinforced. In addition, we provide data to suggest that NO produced by iNOS and nNOS regulates the expression of the vital transcription factors orthodenticle homeobox protein 1 and 2 during an I/R damage.

rat small intestine; ischemia-reperfusion; myenteric plexus; nitric oxide; OTX

INTESTINAL ISCHEMIA-REPERFUSION (I/R) injury from insufficiency of blood flow to all or part of the gastrointestinal tract is associated with high morbidity and mortality (53). The ischemic insult has severe consequences for the metabolically active intestinal mucosa, which undergoes shedding, barrier dysfunction, and bacterial translocation, leading to prolonged reduction in intestinal blood flow (29, 45). Other enteric cell types, including smooth muscle cells, enteric glial cells, and neurons, may also deteriorate (41, 50, 63). Myenteric neurons are especially sensitive and can be irreversibly compromised. The neuronal loss may entail hampered digestion of food (41). Indeed, an I/R injury causes pathological alterations, particularly a slowing of transit, suggestive of a long-lasting neuropathy (55).

Although restoration of blood flow is essential to rescue ischemic tissues, reperfusion induces further cell damage by reactive oxygen species (ROS), with ultimate cell death (44). Nitric oxide (NO) may also play a key role in the cytotoxic events consequent to the I/R damage by diffusion-controlled reaction with another free radical, the anion superoxide, producing peroxynitrite (18). Peroxynitrite may add to overwhelming oxidative protein nitrosylation, DNA breakage, and cell injury (33). Other factors that can amplify damage by reperfusion injury include activation of inflammation at the site of injury (44) and insufficient clearance of dying cells adding to inflammation and further impairing tissue repair (68). NO also takes part in the inflammatory cascade consequent to I/R injury, via indirect, radical-mediated mechanisms, or by direct modulation of proinflammatory protein production via regulation of transcription factors (33, 44).

In the gut, NO is synthesized by the neuronal (n), endothelial (e), and inducible (i) isoforms of nitric oxide synthase (NOS), all of which have been localized to myenteric neurons of different species (19, 62, 66). In the myenteric plexus, nitrergic inhibitory motor neurons and descending interneurons play a fundamental role in the physiological regulation of peristalsis and mainly express nNOS (12). nNOS containing myenteric neurons seem to be selectively targeted by in vivo I/R injury

* V. Filpa and E. Carpanese contributed equally to this work.

Address for reprint requests and other correspondence: C. Giaroni, Dept. of Medicine and Surgery, University of Insubria, via H. Dunant 5, I-21100 Varese, Italy (e-mail: cristina.giaroni@uninsubria.it).

(30, 54). Damage and loss of function of nNOS-immunopositive myenteric neurons may underlie intestinal motility derangement, suggesting that NO produced by nNOS is protective against the metabolic insult (55, 56). Conversely, intestinal I/R damage has been associated with upregulation of iNOS, which may replace nNOS in the synthesis of NO in myenteric neurons (24).

In the present study we aimed to further investigate functional plasticity of nitrergic myenteric neurons occurring in response to an I/R injury by evaluating possible molecular pathways linked to the neuroprotective and neurodamaging action of nNOS and iNOS, respectively. We evaluated the involvement of orthodenticle homeobox protein 1 and 2 (OTX1 and OTX2), belonging to the family of homeoprotein transcription factors, as molecular pathways downstream of nNOS and iNOS activation in myenteric neurons after in vivo I/R damage to the rat small intestine.

Homeobox developmental genes influence neuronal patterning, neurogenesis, and neuronal differentiation during brain development (61). Some of these factors, such as OTX1 and OTX2 continue to be expressed in the adult brain and may function in the development of pathological conditions linked to inflammation and tumorigenesis (14, 31, 51). Homeobox genes are also described to play an important role in the development of intestinal neuromuscular tissues. Alterations of these factors during development may underlay anatomical and/or functional changes of the gut wall, eventually leading to dysmotility in humans (20, 36). In addition, homeobox transcription factors, including OTX, may participate in dysfunctions of intestinal mucosal homeostasis, which occur during inflammatory responses and cancer (13, 69). In our study we aim for the first time to evaluate the possible involvement of OTX proteins in the adaptive responses occurring in myenteric ganglia during an I/R injury in adult rats. The hypothesis of a possible relation and cross regulation among two sources of NOS (nNOS and iNOS), OTX1, and OTX2 was investigated with molecular, morphological, and functional approaches.

METHODS

Animals. Male Wistar rats (Harlan Italy; Correzzana, Monza, Italy), weighing between 250 and 300 g, were housed in groups of four under controlled environmental conditions (temperature 22 ± 2°C; relative humidity 60–70%) with free access to a standard diet and water and were maintained at a regular 12-h:12-h light/dark cycle. Principles of good laboratory animal care were followed and animal experimentation was in compliance with specific national and international laws and regulations. All the experimental procedures were approved by the animal welfare board of the University of Insubria.

Ischemia-reperfusion. Rats were anaesthetized with pentobarbital (50 mg/kg) diluted in sterile phosphate-buffered saline (PBS), given intraperitoneally. After laparatomy, a loop of the small intestine that was supplied by a single branch of the superior mesenteric artery (SMA) was exteriorized and retracted to the left and the SMA was temporarily occluded for 60 min with an atraumatic microvascular clamp. The clip was then gently removed, the abdominal wall was sutured and animals returned to a cage after recovering from anesthesia. In a first set of experiments aiming to validate the model, major histological changes, the degree of inflammatory infiltration and upper gastrointestinal transit efficiency were evaluated after 60 min of ischemia and following 60 min, 24, 48, and 72 h of reperfusion after occlusion. Further experimental animal groups were represented by sham-operated animals undergoing the same surgical manipulation except SMA occlusion and normal unoperated rats. Intestinal specimens obtained from sham-operated were taken 60 min, 24, 48, and 72 h after laparatomy. Since major histological and functional changes have been evidenced at 24 and 48 h after reperfusion (see RESULTS), the successive investigations have been carried out only in these I/R groups, in the respective sham-operated groups and in normal control animals. The following treatments were applied intraperitoneally. Twenty minutes before ischemia or sham operation to four to eight animals of each group: N^{ω}-propyl-L-arginine hydrochloride (NPLA; 10 mg/kg), a selective inhibitor of nNOS (71), and 3-aminomethylbenzylacetamidine dihydrochloride (1400W; 5 mg/kg), a selective inhibitor of iNOS (21). Drugs were diluted in PBS for intraperitoneal administration. Doses were chosen on the basis of literature data indicating the efficacy and absence of toxic activity (34, 37). At the end of the different reperfusion periods, rats were killed by decapitation and segments of the small intestine (8–6 cm long), ~5 cm oral to the ileo-cecal junction, were rapidly excised and rinsed with a physiological ice-cold Tyrode's solution having the following composition (in mM): 137 NaCl, 2.68 KCl, 1.8 $CaCl_2 \cdot 2H_2O$, 2 $MgCl_2$, 0.47 NaH_2PO_4, 11.9 $NaHCO_3$, and 5.6 glucose). Whole wall intestinal segments were fixed and stored for successive immunohistochemistry experiments. Western immunoblot and real-time RT-PCR studies were conducted using preparations consisting of external longitudinal muscle layer segments with attached myenteric plexus (LMMP) obtained immediately after excision of small intestine segments. For RT-PCR experiments, LMMP samples were stored in a preserving solution (RNA later; Ambion Life Technologies Italia, Monza, Italy) at −20°C, while for Western immunoblotting, LMMPs were stored at −80°C for successive assay. Myeloperoxidase activity assay (MPO) was performed on mucosa deprived intestinal segments prepared immediately after excision and frozen at −80°C for storage.

Gastrointestinal transit. Gastrointestinal transit was measured as described by Puig et al. (52), with modifications. In brief, animals were fasted for at least 20 h before the experiment but had free access to water. Small intestine motility was evaluated by measuring the distance traveled by a charcoal meal (0.25 ml of a mixture of 10% vegetable charcoal and 5% arabic gum in saline) administered to each rat by oral gavage, 30 min before death. After this time the abdominal cavity was opened and, after the pylorus and ileo-cecal junction was ligated, the small intestine was carefully removed, avoiding stretching. The distance traveled by black marker along the small intestine was then measured by a premeasured template and was expressed as the percentage of the small intestine length from pylorus to cecum.

Myeloperoxidase activity. Tissue myeloperoxidase (MPO) activity, as an indicator of tissue neutrophil infiltration, was measured according to Bradley et al. (11) with modifications. Mucosa-deprived intestinal samples were homogenized (50 mg/ml) in ice-cold 50 mM potassium phosphate buffer (pH 6.0) containing 0.5% hexadecyl trimethylammonium bromide (HTAB). The homogenate was centrifuged at 14,000 rpm for 20 min at 4°C. The supernatant fraction was recovered and a 34-μl aliquot of the supernatant was mixed with 986 μl of the same phosphate buffer containing 0.167 mg/ml *O*-dianisidine dihydrochloride and 0.0005% hydrogen peroxide. The rate of change in absorbance was recorded spectrophotometrically at 460 nm. One unit (U) of MPO was defined as the amount of enzyme that degrades 1 μmol/min of hydrogen peroxide at 25°C. The results were expressed in units per milligram wet tissue weight.

Histology. Full-thickness small intestine samples were placed in histology cassette, fixed with buffered formalin (4% w/v formaldehyde and acetate buffer 0.05 M) for 24–48 h and routinely embedded in paraffin. Three-micrometer-thick sections were stained with hematoxylin-eosin (HE) for morphologic evaluation. Additional sections were mounted on poly-L-lysine-coated slides for immunohistochemical analysis of neutrophil infiltration. Immunohistochemistry was performed with the avidin-biotin-peroxidase method (32) using a polyclonal antibody anti-MPO (760–2659; Ventana Medical System, Tucson, AZ). Endogenous peroxidase activity was blocked by im-

mersing sections for 10 min in a solution of 3% hydrogen peroxide in water. Primary antibody was incubated overnight at 4°C. Specific biotinylated secondary antibody and avidin-biotin-peroxidase complex were consecutively applied, each for 1 h at room temperature. The immunohistochemical reaction was developed with diaminobenzidine–hydrogen peroxide reaction (65). The sections were counterstained with hematoxylin. Neutrophil infiltration was evaluated only in whole well oriented sections of intestine, counting MPO^+ cells in four high-power fields (×400, diameter 0.55 mm) for each mucosal, sottomucosal, muscular, and serosal-sottoserosal layer. MPO value has been reported as the average of MPO^+ cells for field in each layer.

Whole mount immunohistochemistry. Segments of the rat small intestine were fixed for 4 h at room temperature (RT) in 0.2 mol/l PBS with the following composition (in M): 0.14 NaCl, 0.003 KCl, 0.015 Na_2HPO_4, 0.0015 KH_2PO_4, pH 7.4, 4% formaldehyde, and 0.2% picric acid. Preparations were then cleared of fixative and stored at 4°C in PBS containing 0.05% thimerosal. Whole mounts of LMMPs were then prepared according to the method described by Giaroni et al. (23). Briefly, after specific sites were blocked with PBS containing 1% Triton X-100 and 10% normal horse serum (NHS) (Euroclone; Celbio, Milan, Italy) for 1 h, preparations were incubated with optimally diluted primary antibodies (Table 1). Double-labeling was performed during consecutive incubation times: the first primary antibody was added overnight at 4°C and then incubation with the appropriate secondary antibody followed for 2 h at RT. Whole mounts were successively incubated overnight at 4°C with the second primary antibody and for 2 h at RT with an appropriate secondary antibody. Preparations were mounted onto glass slides, using a mounting medium with DAPI (Vectashield; Vector Laboratory, Burlingame, CA). To establish the proportion of OTX, iNOS, and nNOS expressing myenteric neurons, quantitative analysis of double fluorescently labeled small intestine whole mounts was performed as previously described (22). Briefly, the number of neurons that was immunoreactive for the pan-neuronal marker HUC/D in a ganglion was first counted and then the number of neurons that was immunopositive to the second antibody labeled with a fluorophore of a different color was determined. The cohort size was 10–15 ganglia, and data were collected from preparations obtained from at least 3 animals for each experimental group. Morphological changes in nNOS-immunopositive neurons were evaluated by measuring the total area of the neuronal profile, the ratio of the area of the total cell profile to the cell body profile and the nuclear eccentricity as described by Rivera et al. (54). The cohort size was 20 neurons, and data were collected from whole mounts obtained from at least 3 animals for each experimental group. Negative controls and interference control staining was evaluated by omitting one or both of the primary antibodies or one of the secondary antibodies and by incubating intestinal whole mounts with nonimmune serum from the same species from which primary antibodies were obtained. No specific signal was detected in all these conditions. Preparations were analyzed by confocal microscopy on a Leica TCS SP5 confocal laser scanning system (Leica Microsystems, Wetzlar, Germany) and pictures were processed using Adobe-Photoshop CS2.0 software.

Real-time quantitative RT-PCR. Total RNA was extracted from small intestine LMMPs preparations with TRIzol (Invitrogen) and treated with DNase I (DNase Free; Ambion) to remove any traces of contaminating DNA. cDNA was obtained retrotranscribing 2 μg of total RNA using the High Capacity cDNA synthesis kit (Applied Biosystems, Life Technologies, Grand Island, NY). Quantitative RT-PCR was performed on the Abi Prism 7000 real-time thermocyclator (Applied Biosystems) with Power Sybr Green Universal PCR Master Mix (Applied Biosystems) following manufacturer's instructions. Primers were designed using Primer Express software (Applied Biosystems) on the basis of available sequences deposited in public database (Table 2). For quantitative RT-PCR a final concentration of 500 nM for each primer was used. Primers were designed to have a similar amplicon size and similar amplification efficiency as required for the utilization of the $2^{-\Delta\Delta Ct}$ method to compare gene expression (43). β-Actin was used as housekeeping gene. Experiments were performed four to eight times for each different preparation. The effect of the drug tested on the different experimental groups was evaluated by comparing the respective $2^{-\Delta\Delta Ct}$ values.

Western immunoblot analysis. OTX1, OTX2, iNOS, and nNOS protein level analysis was carried out starting from LMMPs preparations with successive centrifugations according to the method described by Giaroni et al. (22). The purified membrane fraction and the

Table 1. *Primary and secondary antisera and their respective dilutions used for Western blot assay and immunohistochemistry*

Antiserum	Dilution (WB)	Dilution (HC)	Source	Host Species
Primary antisera				
iNOS	1:300	1:50	Santa Cruz Biotechnology (sc8310; H-174)	Rabbit
iNOS		1:50	AbCam (ab49999)	Mouse
nNOS		1:200	Millipore (AB1529)	Sheep
nNOS	1:200	1:50	Santa Cruz Biotechnology (sc648; R-20)	Rabbit
OTX pan		1:100	Santa Cruz Biotechnology (sc11026; N-15)	Goat
OTX1	1:200	1:50	Santa Cruz Biotechnology (sc133872; Y-22)	Rabbit
OTX2	1:200	1:50	Santa Cruz Biotechnology (sc30659; P-15)	Goat
HUC/D		1:100	Molecular Probes (A-21272)	Mouse
S-100		1:200	Dako (Z0311)	Rabbit
β-actin	1:1,000			Mouse
Secondary antisera and streptavidin complexes				
Anti-rabbit Alexa Fluor 488		1:200	Molecular Probes (A21206)	Donkey
Anti-goat Cy3		1:500	Jackson ImmunoResearch Laboratories (705-165-147)	Donkey
Cy3-conjugated streptavidin		1:500	Amersham (PA43001)	
FITC-conjugated straptavidin		1:200	Molecular Probes (SA1001)	
$F(ab')_2$ anti-mouse IgG (H+L) biotin		1:300	Caltag Laboratories (M35015)	Goat
$F(ab')_2$ anti-rabbit IgG (H+L) biotin		1:300	Caltag Laboratories (L43015)	Goat
Anti-rabbit IgG HRP peroxidase conjugated	1:10,000		Santa Cruz Biotechnology (sc2004)	Goat
Anti-goat IgG HRP peroxidase conjugated	1:7,500		Santa Cruz Biotechnology (sc2020)	Donkey

iNOS, inducible nitric oxide synthase; nNOS, neuronal nitric oxide synthase; WB, Western blot assay; HC, immunohistochemistry; OTX1 and OTX2, orthodenticle homeobox protein 1 and 2. Company locations: Amersham, GE Healthcare, Buckinghamshire, UK; Caltag Laboratories, Invitrogen, Burlingame, CA; Cell Signaling Technology, Danvers, MA; Dako, Glostrup, Demark; Jackson ImmunoResearch Laboratories, Baltimore, MD; Molecular Probes, Carlsbad, CA; Santa Cruz Biotechnology, Santa Cruz, CA; Sigma-Aldrich, Milan, Italy.

Table 2. *Sequence of primers used in the study for qRT-PCR analysis*

Gene	Sequence
β-Actin	
Forward	5′-AGGCCCCTCTGAACC-3′
Reverse	5′-GGGGTGTTGAAGGTC-3′
iNOS	
Forward	5′-CACTTTGACGACTCA-3′
Reverse	5′-AGCGAACAAATAGA-3′
nNOS	
Forward	5′-ACAGTCATCAGACAC-3′
Reverse	5′-GGGCAGCAACGGGAT-3′
OTX1	
Forward	5′-GCGAGGAGGTGGCTCTCA-3′
Reverse	5′-GGCTCGGCGGTTCTTGA-3′
OTX2	
Forward	5′-CCCAATTTGGGCCGACTT-3′
Reverse	5′-GCGTAAGGCGGTTGCTTTAG-3′
VEGFα	
Forward	5′-GCTGTGTGTGTGAGTGGCTTA-3′
Reverse	5′-CCCATTGCTCTGTACCTTGG-3′
HIF1α	
Forward	5′-AAGCACTAGACAAAGCTCACCTG-3′
Reverse	5′-TTGACCATATCGCTGTCCAC-3′

HIF1α, hypoxia-inducible factor-1α; VEGFα, vascular endothelial growth factor-α.

supernatant were boiled for 2 min after dilution with Laemmli sample buffer and processed as described elsewhere (39). Membranes were incubated with optimally diluted primary and horseradish peroxidase-conjugated secondary antisera (Table 1). OTX1, OTX2, and iNOS levels were evaluated in the supernatant (cytosolic) fraction, whereas nNOS levels were investigated in the membrane fraction. Blots for OTX1, OTX2, iNOS, and nNOS were developed using an enhanced chemiluminescence technique (ECL advance Amersham Pharmacia Biotech, Cologno Monzese, Italy). Signal intensity was quantified by densitometric analysis using ImageJ National Institutes of Health image software (downloadable at https://imagej.nih.gov/). (59). In each membrane β-actin was monitored and used as protein loading control. Experiments were performed four to seven times for each different preparation. The effect of in vivo I/R on protein levels was expressed as the percentage variation vs. values obtained in preparations deriving from control normal unoperated animals. Specificity of iNOS and nNOS primary antibodies was evaluated by testing their selectivity in RAW 264.7 macrophage cells and in the rat hippocampus, respectively (data not shown). Specificity of OTX1 and OTX2 primary antibodies was evaluated by testing their selectivity in the spontaneous immortalized human Müller cell line (MIO-M1) (40) and in the rat hippocampus (42), respectively (data not shown). Omission of the primary antibody was also performed as a control of specificity.

Statistical analysis. For statistical analysis the GraphPad Instat statistical package (version 5.3, GraphPad software, San Diego, CA) was used. Data were analyzed by one-way ANOVA followed, when significant, by an appropriate post hoc comparison tests (Tukey's multiple comparisons tests). Differences were considered statistically significant when $P \leq 0.05$.

Drugs and materials. N^5-[imino(propylamino)methyl]-L-ornithine hydrochloride [N^{ω}-propyl-L-arginine hydrochloride (NPLA)] and 3-aminomethylbenzylacetamidine dihydrochloride (1400W) were purchased from Tocris (Bristol, UK). All other reagents were purchased either from Sigma-Aldrich or from Bio-Rad (Segrate, Italy).

RESULTS

General observations: histology. Occlusion of the terminal branch of the SMA induced a change in the color of the corresponding intestinal segment that became purple. After blood flow restoration the tissue returned to a normal pink color. Animals recovered uneventfully from anesthesia and once awake were active and ate normally. No signs of distress could be detected. A gross visual inspection of the regions subjected to I/R did not reveal any anomaly with respect to sham-operated and unoperated control animals at all times.

The microscopic evaluation of intestinal sections showed signs of cellular suffering both in neuronal and muscle cells. At 24 and 48 h after reperfusion many neurons of submucosal and myenteric plexus were swollen with cytoplasm vacuolisations and ill-defined cellular membrane with respect to normal control preparations (Fig. 1, *A* and *B*). Nuclear inclusions were sometimes present. Cytoplasmic vacuolisations and spaces between muscle cells were the main degenerative changes observed in some regions of muscularis propria with respect to normal control preparations (Fig. 1, *A* and *B*). Mucosa and serosal epithelium did not display prominent histological abnormalities. In sham-operated samples the histological features of cellular suffering previously described were rarely observed in neurons or muscle cells.

Neutrophil infiltration and MPO. Neutrophils, evaluated by the MPO reaction, were counted in three compartments: the mucosa, the submucosa, and the muscularis propria (Figs. 1*C* and 2, *A–C*). In the mucosa, no significant variation in the number of MPO-positive cells per field was observed after both I/R and in sham-operated animals with respect to normal control preparations. In the submucosa, a significant increase in neutrophil infiltration was observed both after 24 h of reperfusion and in the respective sham-operated group ($P < 0.05$ and $P < 0.01$, respectively) with respect to normal values. A significant increase of MPO reaction was also observed in the sham-operated group, 48 h after laparatomy ($P < 0.05$). In the muscularis propria, a significant increase in the number of neutrophil cells per field was observed after 24 h of reperfusion ($P < 0.01$) with respect to normal preparations. Neutrophil number increased, although not significantly, 48 and 72 h following reperfusion with respect to normal values. In the 24, 48, and 72 h sham-operated groups the numbers of neutrophils increased, but not significantly, with respect to normal preparations.

In mucosa-deprived rat small intestine segment, MPO activity significantly increased after 60 min, 24, and 48 h of reperfusion ($P < 0.05$ and $P < 0.01$) with respect to values obtained in normal conditions. In preparations obtained from sham-operated animals, MPO activity significantly increased ($P < 0.05$) after 24 and 48 h of reperfusion. MPO values returned to normal values 72 h following reperfusion and in the respective sham-operated group (Fig. 3*A*).

In normal control animals, in vivo treatment with NPLA and 1400W did not modify MPO activity. Both NPLA and 1400W significantly reduced ($P < 0.01$) I/R-induced enhancement of MPO after both 24 and 48 h of reperfusion and in the respective sham-operated animal. In preparations obtained from sham-operated animals enhancement of MPO activity after 24 and 48 h of reperfusion was significantly reduced ($P < 0.05$) by both NPLA and 1400W (Fig. 3*B*).

Gastrointestinal transit. Upper gastrointestinal transit (Fig. 4*A*) significantly decreased 60 min ($P < 0.05$) after in vivo-induced ischemia and returned toward control values 60 min after reperfusion. A delay of transit was observed at 24 h,

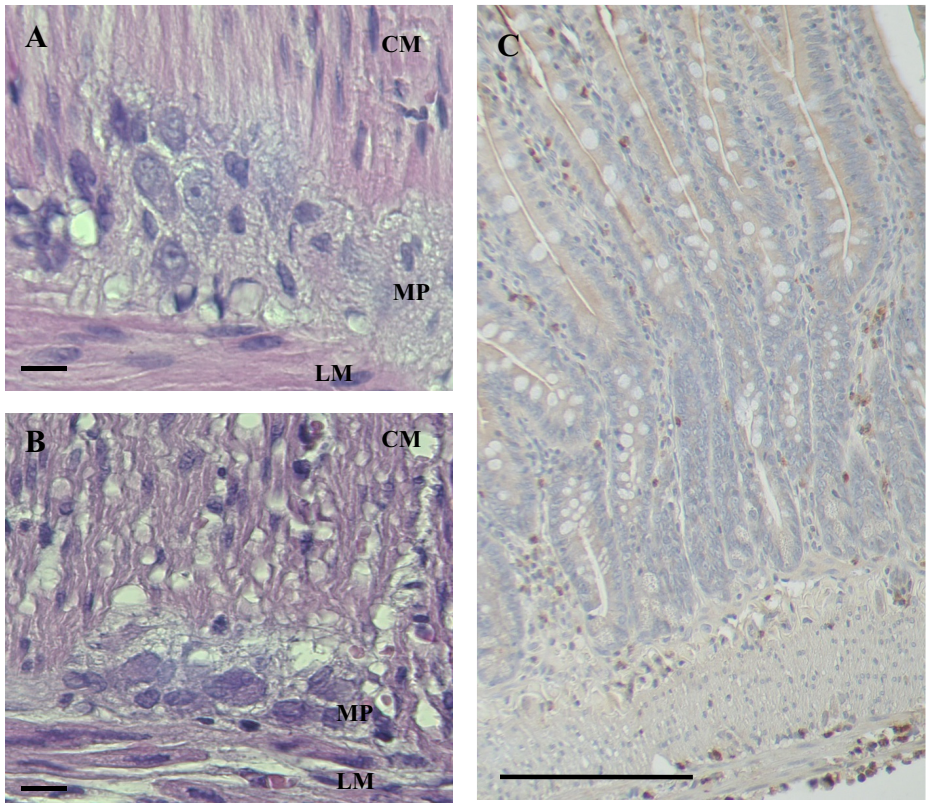

Fig. 1. *A*: smooth muscle cells in the circular (CM) and longitudinal (LM) layers and myenteric plexus (MP) of normal control rat small intestine [hematoxylin-eosin (HE); original magnification: ×600; bar: 0.01 mm]. *B*: smooth muscle cells in the CM and LM layers and MP of rat small intestine obtained after 60 min of in vivo ischemia followed by 24 h of reperfusion. Neurons and muscle cells show signs of cellular suffering. In particular, neurons display irregular and ill-defined nuclear and cellular membrane, whereas cytoplasmic vacuolizations and spaces between cells are present in muscle tissue (HE; original magnification: ×600; bar: 0.01 mm). *C*: myeloperoxidase (MPO) immunohistochemical staining of whole wall rat small intestine obtained after 60 min of in vivo ischemia followed by 24 h of reperfusion. Neutrophils are well marked (brown) and their count is easy for all the layers.

which became significant ($P < 0.01$) following 48 h of reperfusion. After 72 h of reperfusion transit was lower, but not significantly different, with respect to normal control values. In sham-operated groups, at all times investigated, transit was reduced, although not significantly, with respect to values obtained in normal control animals.

NPLA significantly delayed transit in normal control animals (Fig. 4*B*), in the 48-h sham-operated group ($P < 0.05$), and after 48 h of reperfusion following ischemia ($P < 0.001$). In this latter group NPLA further, although not significantly, reduced the delay of transit induced by the I/R injury. In normal control animals and in the 48-h sham-operated group, in vivo treatment with 1400W did not modify gastrointestinal transit. The reduction of transit observed after 48 h of reperfusion was completely restored to normal control values after 1400W administration.

Hypoxia-inducible factor-α and vascular endothelial growth factor-α mRNA levels in LMMP preparations. Hypoxia-inducible factor (HIF1α) and vascular endothelial growth factor (VEGFα) mRNA levels in rat small intestine LMMP preparations obtained from normal animals, after 24 and 48 h of reperfusion following ischemia, and in the relative sham-operated animals are described in Fig. 5, *A* and *B*, respectively. HIF1α mRNA levels significantly increased after 24 h of reperfusion and in the relative sham-operated group with respect to normal animals ($P < 0.001$ and $P < 0.05$, respectively). Both enhancements decreased 48 after ischemia and in the respective sham-operated group. At this time HIF1α mRNA levels were not significantly different with respect to normal control levels. VEGFα gene expression was also significantly upregulated 24 h after reperfusion but not in the respective sham-operated group ($P < 0.001$ and $P < 0.05$, respectively). After 48 h of reperfusion and in the respective sham-operated group, the levels of VEGFα transcript were not significantly different with respect to control values.

Levels of nNOS and iNOS mRNA in LMMP preparations. Quantitative RT-PCR analysis of nNOS and iNOS mRNA in rat small intestine LMMP preparations is shown in Fig. 6, *A* and *B*. After 24 and 48 h of reperfusion following the ischemic injury, the levels of nNOS mRNA did not significantly change with respect to both normal and the respective sham-operated animals. Administration of NPLA and 1400W did not modify nNOS mRNA levels in all experimental groups studied (Fig. 6*A*). iNOS mRNA levels significantly increased after 24 and 48 h of reperfusion following in vivo ischemia with respect to preparations obtained from both normal ($P < 0.001$) and from the respective sham-operated groups ($P < 0.001$ and $P < 0.05$). In the sham-operated groups, iNOS mRNA levels increased, although not significantly, with respect to preparations obtained from normal animals. In preparations obtained from both normal and sham-operated animals, iNOS mRNA levels remained unchanged after administration of both 1400W and NPLA. I/R-induced enhancement of iNOS mRNA levels at 24 and 48 h of reperfusion were reduced, but not significantly, by 1400W. Pretreatment with NPLA did not affect iNOS mRNA levels both at 24 and 48 h after reperfusion (Fig. 6*B*).

Levels of expression of nNOS and iNOS in LMMP preparations. Western blot analysis of nNOS and iNOS protein expression in rat small intestine LMMP preparations is shown in Fig. 4, *C* and *D*. In rat small intestine LMMP preparations, the nNOS-specific antibody revealed one band at 155 kDa (Fig. 6*C*). In I/R conditions and in sham-operated animals, nNOS protein levels remained unchanged with respect to normal animals (Fig. 4*C*). Both NPLA and 1400W did not significantly

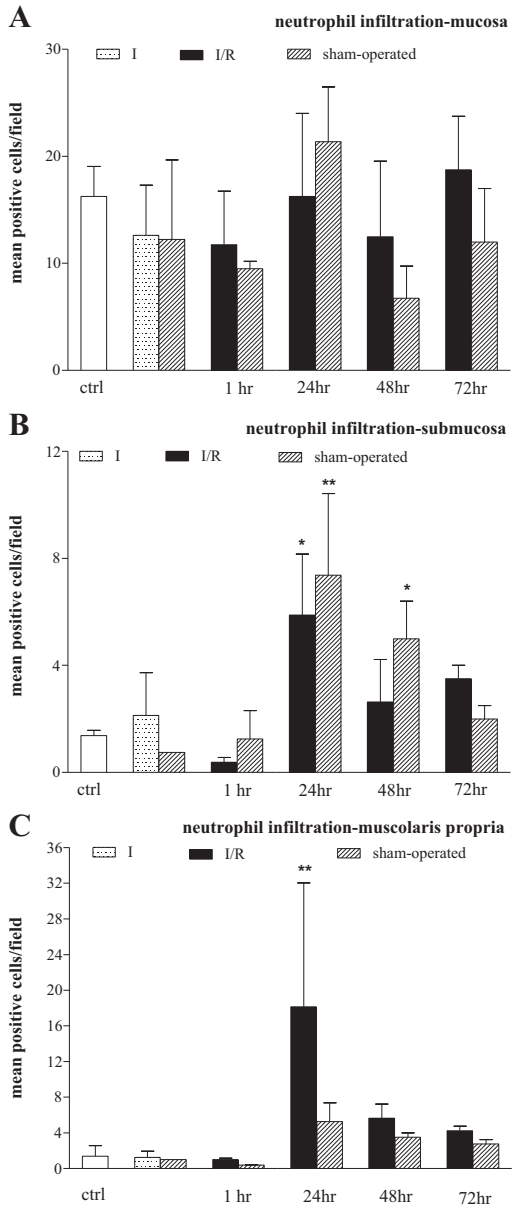

Fig. 2. Characterization of neutrophil infiltrate in the intestinal wall after ischemia-reperfusion (I/R) injury expressed as number of neutrophils in the rat small intestine mucosa (*A*), submucosa (*B*), and muscolaris propria (*C*) of normal control animals (empty bar), after 60 min of in vivo ischemia (dotted bar), at different times after inducing in vivo I/R (solid bars), and in the respective animals subjected to sham operation (slashed bars). Values are expressed as means ± SD of neutrophil count of 4–5 experiments. $^{*}P < 0.05$, $^{**}P < 0.01$ by one-way ANOVA followed by Tukey's test vs. values obtained in normal control animals.

modify nNOS protein expression in all experimental groups (Fig. 6*C*). In rat small intestine LMMP preparations (Fig. 6*D*), the specific antibody against iNOS revealed one band at 125 kDa. iNOS protein levels significantly increased ($P < 0.01$) with respect to normal animals 24 h after reperfusion and further significantly raised ($P < 0.001$) at 48 h after reperfusion following in vivo ischemia (Fig. 6*D*). iNOS protein levels at 48 h were also significantly higher than the levels observed in the respective sham-operated group ($P < 0.001$). In sham-operated groups, both at 24 and 48 h after laparatomy, iNOS protein levels did not significantly change with respect to normal animals. After in vivo treatment with NPLA, iNOS protein levels remained unchanged in all experimental groups. 1400W significantly reduced I/R-induced enhancement of iNOS protein levels, both at 24 and 48 h after reperfusion ($P < 0.05$ and $P < 0.001$, respectively; Fig. 6*D*).

Levels of OTX1 and OTX2 mRNA in LMMP preparations. OTX1 and OTX2 mRNA levels in rat small intestine LMMP preparations obtained from the different experimental groups are described in Fig. 7, *A* and *B*. OTX1 mRNA levels significantly increased 24 and 48 h after in vivo ischemia with respect to both normal and sham-operated animals ($P < 0.001$). In preparations obtained from sham-operated animals, OTX1 mRNA levels increased, although not significantly, with respect to normal animals. Treatment with both NPLA and 1400W did not significantly change OTX1 mRNA levels in preparations obtained from both normal and sham-operated animals. Enhancement of OTX1 gene expression at both 24 and 48 h of reperfusion after in vivo ischemia was significantly reduced by both NPLA ($P < 0.05$ and $P < 0.001$, respectively) and 1400W ($P < 0.01$ and $P < 0.001$, respectively) (Fig. 7*A*). OTX2 mRNA levels significantly increased after 24 h of

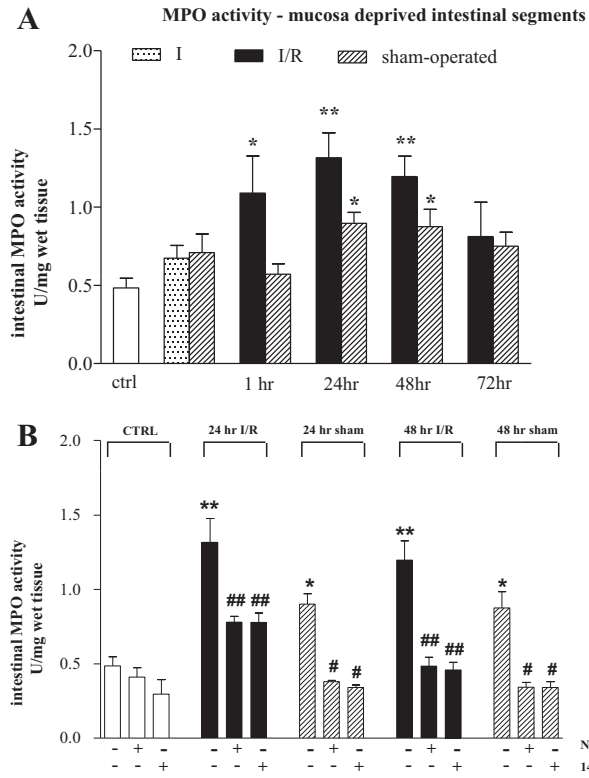

Fig. 3. MPO activity measured in mucosa-deprived intestinal segments and effect of neuronal and inducible nitric oxide synthase (nNOS and iNOS) blockade. *A*: MPO activity in normal control animals (empty bar), after 60 min of in vivo ischemia (dotted bar), at different times after inducing in vivo I/R (solid bars), and in the respective animals subjected to sham-operation (slashed bars). *B*: effect of N^{ω}-propyl-L-arginine hydrochloride (NPLA) and 1400W on MPO activity in control animals (empty bar), after 60 min of in vivo ischemia followed by 24 and 48 h of reperfusion (solid bars) and in the respective sham-operated animals (slashed bars). Treatments are specified below graph. Values are expressed as means ± SE of MPO activity of 4–9 experiments. $^{*}P < 0.05$, $^{**}P < 0.01$ vs. values obtained in normal control animals; $^{\#}P < 0.05$, $^{\#\#}P < 0.01$ vs. values obtained in the respective I/R or sham-operated group by one-way ANOVA followed by Tukey's test.

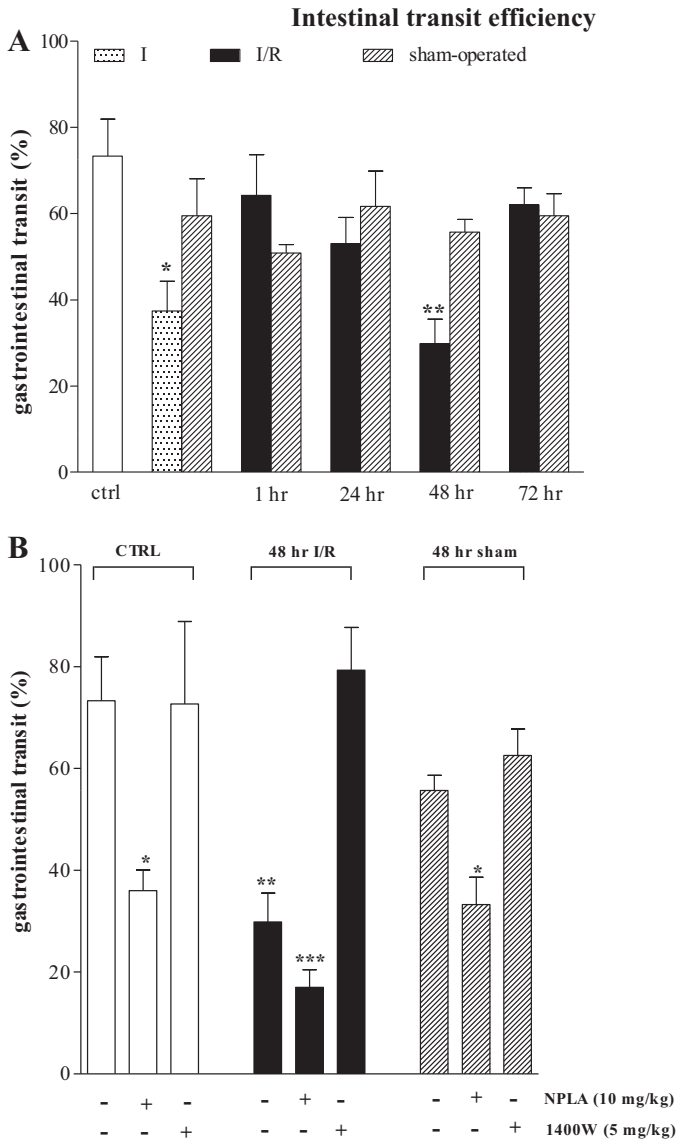

Fig. 4. Evaluation of the efficiency of small intestine transit during I/R and effect of iNOS and nNOS blockade. *A*: gastrointestinal transit in control animals (empty bar), after 60 min of in vivo ischemia (dotted bar), at different times after inducing in vivo I/R (solid bars), and in the respective animals subjected to sham-operation (slashed bars). *B*: effect of 1400W and NPLA, iNOS and nNOS inhibitors, respectively, on gastrointestinal transit in control animals (empty bar), after 60 min of in vivo ischemia followed by 24 and 48 h of reperfusion (solid bars) and in the respective sham-operated animals (slashed bars). Treatments are specified below graph. Values are expressed as means ± SE of the gastrointestinal transit of 4–8 experiments. $*P < 0.05$, $**P < 0.01$, $***P < 0.001$ by one-way ANOVA followed by Tukey's test vs. values obtained in normal animals.

reperfusion ($P < 0.001$) and declined toward values obtained in normal preparations after 48 h of reperfusion. OTX2 gene expression was also significantly upregulated in sham-operated animals 24 h after laparatomy ($P < 0.05$) but remained unchanged at 48 h with respect to normal values. Both NPLA and 1400W did not significantly modify OTX2 mRNA levels in preparations obtained from normal animals, 24-h sham-operated animals, after 48 h of reperfusion and in the respective sham-operated group. NPLA and 1400W significantly ($P < 0.001$) decreased OTX2 mRNA levels induced by 24 h of reperfusion following in vivo ischemia (Fig. 7*B*).

Levels of expression of OTX1 and OTX2 in LMMP preparations. In rat small intestine LMMP preparations (Fig. 7*C*), the specific OTX1 antibody revealed one band at 37 kDa. Since RT-PCR analysis revealed a prominent enhancement of OTX1 mRNA at 48 h after reperfusion, OTX1 protein levels were analyzed in protein extracts of LMMPs obtained at this time of reperfusion and in the respective sham-operated group. OTX1 protein expression significantly increased ($P < 0.01$) after 48 h of reperfusion following in vivo ischemia and remained unchanged in sham-operated preparations. Administration of both NPLA and 1400W did not alter OTX1 protein expression in normal and in sham-operated animals. NPLA and 1400W significantly reduced I/R-induced OTX1 protein enhancement at this time ($P < 0.001$ and $P < 0.05$, respectively) (Fig. 7*C*).

In rat small intestine LMMP preparations (Fig. 7*D*), the specific antibody revealed one band at 32 kDa. Since OTX2 mRNA significantly increased 24 h after reperfusion, OTX2 protein levels were analyzed in protein extracts of LMMP obtained at this time of reperfusion and in the respective

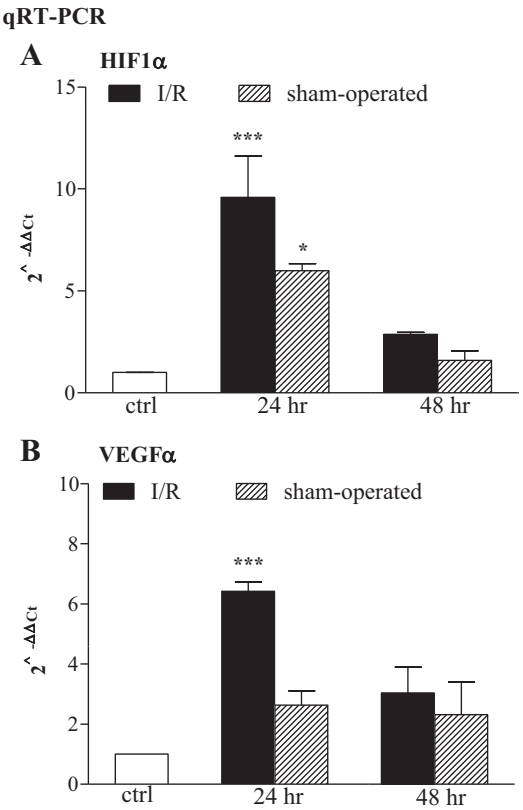

Fig. 5. RT-PCR quantification of hypoxia-inducible factor (HIF1α) and VEGFα transcripts in rat small intestine longitudinal muscle myenteric plexus preparations during in vivo I/R. *A*: HIF1α mRNA levels in control animals (empty bar), at 24 and 48 h after inducing in vivo I/R (solid bars), and in sham-operated animals (slashed bars). *B*: VEGFα mRNA levels in control animals (empty bar), at 24 and 48 h after inducing in vivo I/R (solid bars) and in sham-operated animals (slashed bars). Values are means ± SE of 4–5 experiments of the percentage variation of relative gene expression with respect to values obtained in control (empty bar). $*P < 0.05$, $***P < 0.001$ by one-way ANOVA followed by Tukey's test. The relative gene expression was determined by comparing $2^{-\Delta\Delta Ct}$ values normalized to β-actin.

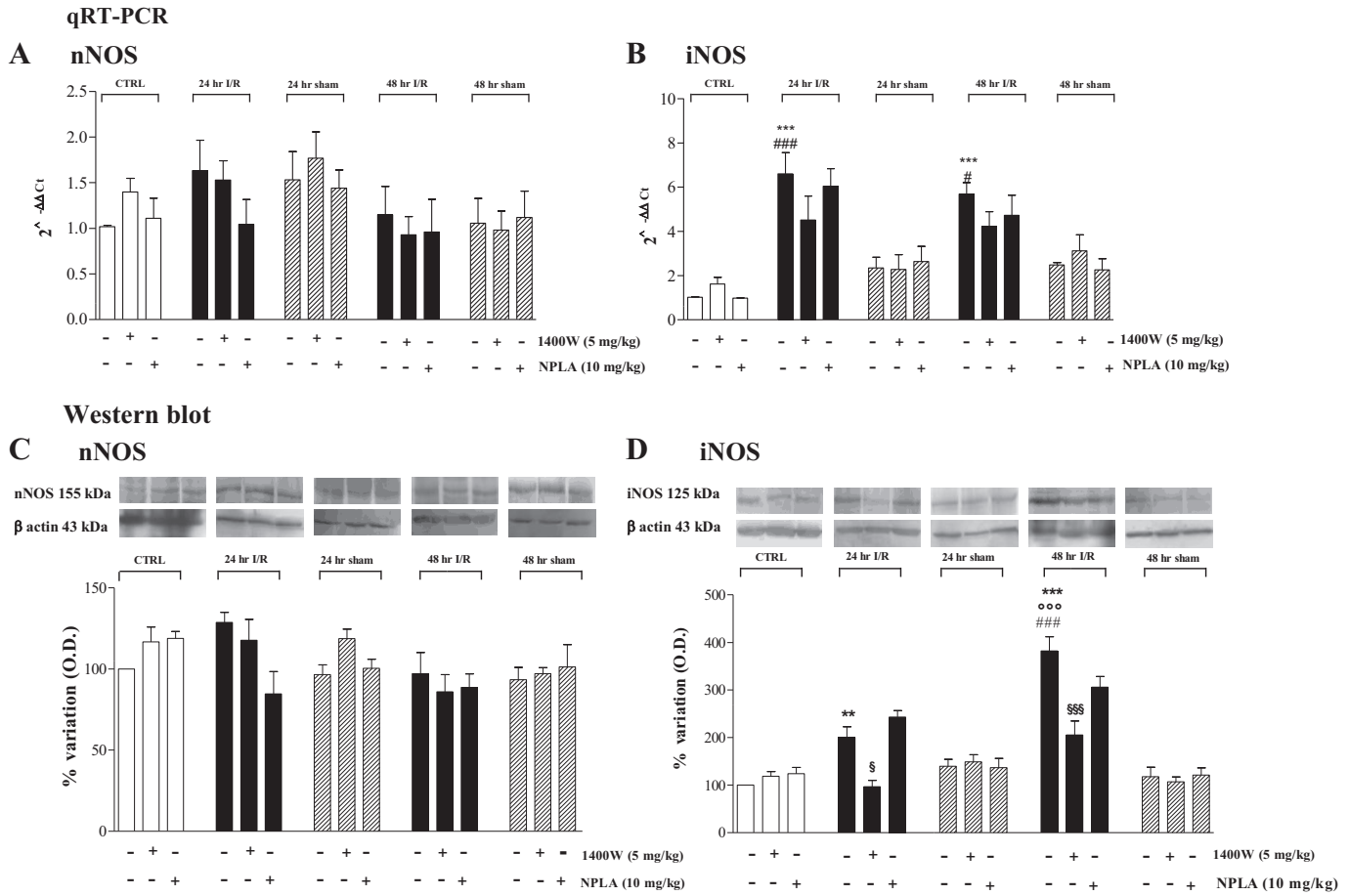

Fig. 6. RT-PCR and Western blot analysis of nNOS and iNOS transcript and protein levels in rat small intestine longitudinal muscle myenteric plexus preparations (LMMPs) during in vivo I/R. nNOS (*A*) and iNOS (*B*) mRNA levels in control animals (empty bar), at 24 and 48 h after inducing I/R (solid bars), and in the respective sham-operated animal (slashed bars). The relative gene expression was determined by comparing $2^{-\Delta\Delta Ct}$ values normalized to β-actin. Values are means ± SE of 4–8 experiments of the percentage variation of relative gene expression with respect to values obtained in control animals. Levels of protein expression of nNOS (*C*) and iNOS (*D*) were obtained in the membrane and supernatant fractions of LMMPs, respectively. Blots representative of immunoreactive bands for nNOS and iNOS and β-actin in the different experimental conditions are reported on top of *C* and *D*. Samples (100 μg) were electrophoresed in SDS-10% polyacrylamide gels. Numbers at the margins of the blots indicate relative molecular weights of the respective protein in kDa. Specific treatments are reported below graphs. Values are expressed as means ± SE of 4–7 experiments of the percentage variation of optical density (O.D.) with respect to values obtained in control. $^{**}P < 0.01$, $^{***}P < 0.001$ vs. control animals; $^{\circ\circ\circ}P < 0.001$ vs. 24 h of I/R group; $^{\#}P < 0.05$, $^{\#\#\#}P < 0.001$ vs. respective sham-operated group; $^{\S}P < 0.05$, $^{\S\S\S}P < 0.01$ vs. respective I/R group by one-way ANOVA followed by Tukey's test.

sham-operated group. OTX2 expression significantly increased after 24 h of reperfusion following in vivo ischemia ($P < 0.001$) and remained unchanged in sham-operated preparations with respect to normal animals. In all experimental groups NPLA reduced OTX2 protein levels. However, a statistically significant reduction was observed only at 24 h of reperfusion after ischemia and in the sham-operated group ($P < 0.001$ and $P < 0.01$, respectively). In normal and sham-operated animals, 1400W did not modify OTX2 protein levels. The iNOS blocker significantly reduced OTX2 protein expression after 24 h of reperfusion following in vivo ischemia ($P < 0.05$) reperfusion (Fig. 7*D*).

Distribution of nNOS-immunoreactive and iNOS-immunoreactive in LMMP whole mounts preparations. In preparations obtained from all experimental groups, nNOS-immunoreactive was observed in the cytoplasm of myenteric neurons. Some neurons had a large cell body with club-like dendrites, while others were small with an ovoidal shape and with no visible dendrites. nNOS-immunoreactive was evidenced also in neuronal fibers within the ganglia and along the interconnecting strands and in the secondary and tertiary fiber tracts. (Fig. 8, *A* and *D*). The number of nNOS-immunoreactive myenteric neurons in LMMP preparations obtained from normal animals was 21.8 ± 2.8%, ($n = 4$) and was not significantly different with respect to the values obtained at 24 and 48 h following the ischemic damage and to the relative sham-operated groups (Fig. 9*A*). However, the profiles of myenteric neurons staining for nNOS were altered in small intestine specimens collected after 24 and 48 h of reperfusion. Following 24 and 48 h after I/R, the total cell area and the ratio between the total cell area and the cell soma area were significantly larger with respect to both normal and sham-operated animals ($P < 0.001$ and $P < 0.05$, respectively; Fig. 10, *A* and *B*). nNOS-immunoreactive neurons of both I/R preparations significantly displayed more nuclear eccentricity, which is indicative of damage, with respect to both normal and sham-operated animals ($P < 0.001$ and $P < 0.05$, respectively) (Fig. 10*C*). Total cell area, area ratios, and nuclear eccentricity

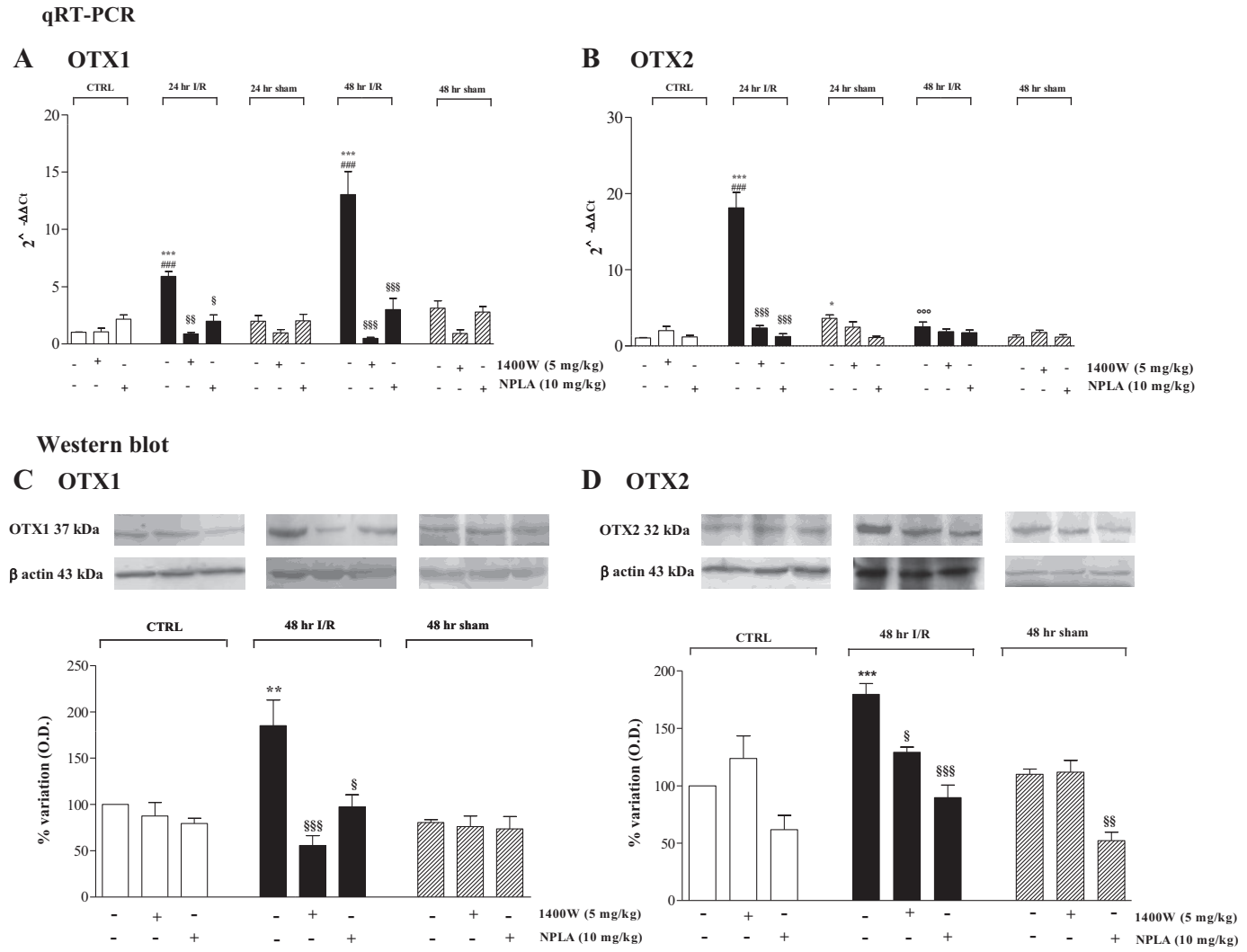

Fig. 7. RT-PCR and Western blot analysis of orthodenticle homeobox protein 1 and 2 (OTX1 and OTX2) transcript and protein levels in rat small intestine longitudinal muscle myenteric plexus preparations (LMMPs) after in vivo I/R damage. RT-PCR quantification of OTX1 (*A*) and OTX2 (*B*) transcripts in control animals (empty bar), at 24 and 48 h after inducing I/R (solid bars), and in the respective sham-operated animal (slashed bars).Values are mean ± SE of 4–8 experiments of the percentage variation of relative gene expression with respect to values obtained in control animals. The relative gene expression was determined by comparing $2^{-\Delta\Delta Ct}$ values normalized to β-actin. Levels of OTX1 (*C*) and OTX2 (*D*) protein expression analyzed in supernatant fractions of LMMPs obtained at 24 and 48 h after inducing I/R, respectively, and in related sham-operated groups and in control animals. Blots representative of immunoreactive bands for OTX1 and OTX2 and β-actin in the different experimental conditions are reported at *top* of *C* and *D*. Samples (100 μg) were electrophoresed in SDS-10% polyacrylamide gels. Numbers at the margins of the blots indicate relative molecular mass of the respective protein in kDa. Values are expressed as means ± SE of 4–7 experiments of the percentage variation of optical density (O.D.) with respect to values obtained in normal animals. Specific treatments are reported below graphs. $^{**}P < 0.01$ $^{***}P < 0.001$ vs. control animals; $^{\circ\circ\circ}P < 0.001$ vs. 24 h of I/R group; $^{\#\#\#}P < 0.001$ vs. respective sham-operated group; $^{\S}P < 0.05$, $^{\S\S\S}P < 0.001$ vs. respective I/R or sham-operated group by one-way ANOVA followed by Tukey's test.

of myenteric neurons staining for nNOS were not significantly different in preparations obtained from normal and sham-operated animals (Fig. 10, *A–C*).

In LMMP preparations obtained from all experimental groups, iNOS staining was observed in the soma of myenteric neurons with an ovoidal shape and no visible dendrites (Fig. 8, *G* and *J*). In control animals, the percentage of iNOS-immunoreactive neurons was 5.2 ± 0.6%, $n = 6$. The proportion of iNOS-immunopositive neurons significantly increased 24 and 48 h after ischemia (11.6 ± 1.3%, $n = 5$, $P < 0.001$, and 11.7 ± 0.8%, $n = 6$, $P < 0.001$, respectively), with respect to the value obtained in control animals. The number of myenteric neurons staining for iNOS in the myenteric plexus of sham-operated animals was not significantly different with respect to control values (Fig. 9*B*). Double labeling with S100 revealed the presence of iNOS-immunoreactivity in enteric glial cells both in myenteric ganglia and in the muscular layer (Fig. 8, *M–O*).

Distribution of OTX1-immunoreactive and OTX2-immunoreactive in LMMP whole mounts preparations. In preparations obtained from all experimental groups, pan OTX-immunoreactivity was observed in the cytoplasm and nucleus of myenteric neurons as well as in prolongations surrounding neuronal membranes. Some neurons had a large cell body, while other smaller neurons with an ovoidal shape were prevalently localized in the periphery of the ganglion (data not shown). In control animals, the percentage of pan OTX-immunoreactive neurons was 5.7 ± 0.4%, $n = 6$. The proportion of pan-OTX-

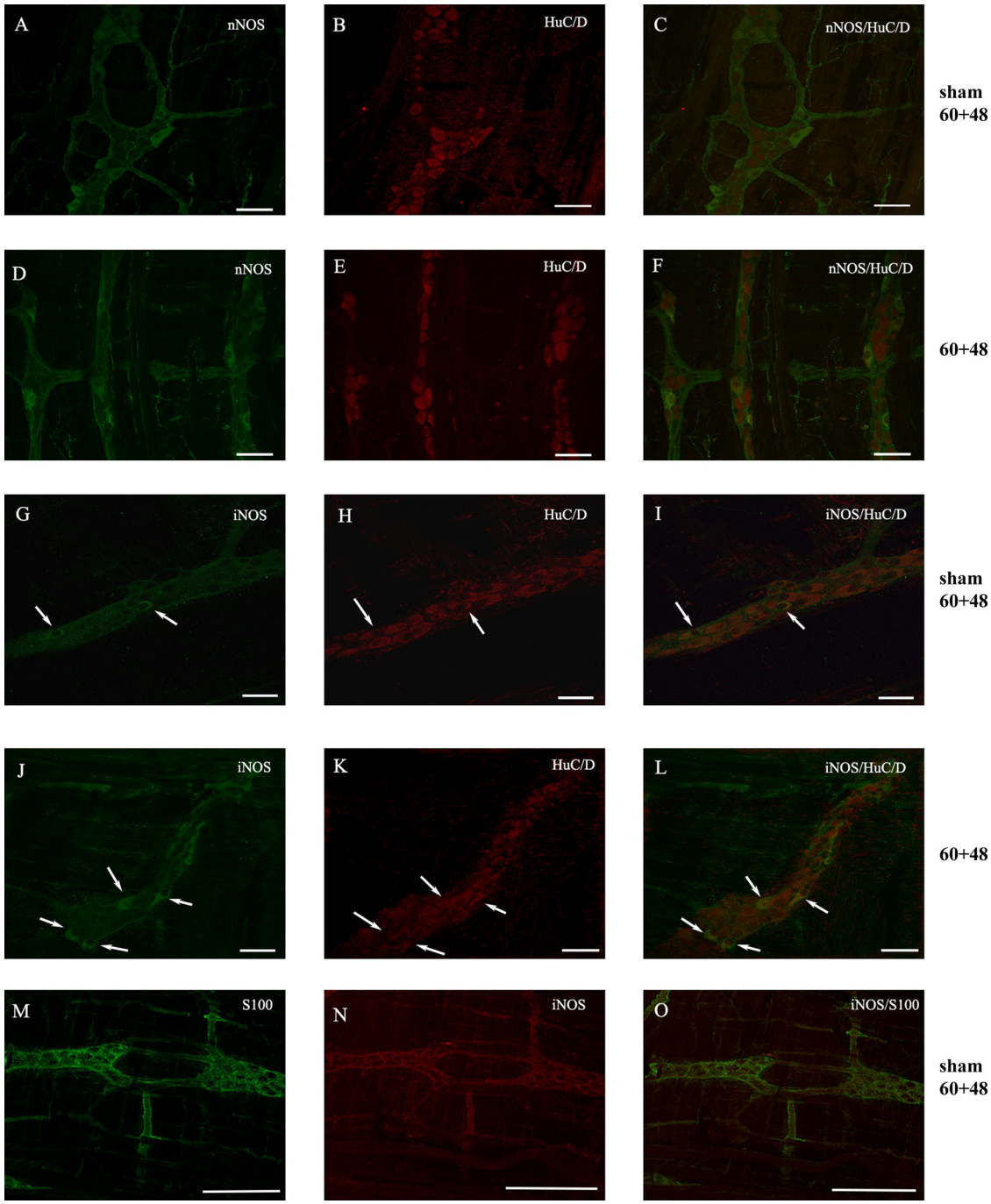

Fig. 8. Immunohistochemical localization of nNOS and iNOS in whole mount preparations of the rat small intestine obtained from animals subjected to in vivo ischemia followed by 48 h reperfusion and in the relative sham-operated group. *A–F*: colocalization of nNOS with the neuronal marker HUC/D. *G–L*: colocalization of iNOS with HUC/D. The neuronal marker HUC/D stained the somata of all myenteric neurons (*B*, *E*, *H*, and *K*). *M–O*: colocalization of iNOS with the glial marker S100. Arrows indicate iNOS- and HUC/D-positive myenteric neurons (*G–L*). Bar = 50 μm.

immunopositive neurons significantly increased 24 and 48 h after ischemia (17.0 ± 1.6%, $n = 6$, $P < 0.001$, and 17.3 ± 0.8%, $n = 6$, $P < 0.001$, respectively), with respect to the value obtained in control animals (Fig. 9*C*). The number of myenteric neurons staining for pan-OTX antibody in the myenteric plexus of sham-operated animals was not significantly higher (10.0 ± 1.4%, $n = 4$ $P < 0.05$, 11.0 ± 0.6%, $n = 4$ $P < 0.01$, respectively) with respect to control values (Fig. 9*C*). Double staining of both OTX1 and OTX2 specific antibodies with S100 showed localization of OTX1 immunoreactivity in the enteric glial network (Fig. 11, *B–D*), while OTX2 immunoreactivity could not be evidenced at this level (data not shown). Double staining with specific antibodies directed against either OTX1 or OTX2 and HUC/D showed that few myenteric neurons are immunoreactive to OTX1 (data not shown), while OTX2 has a predominant neuronal localization (Fig. 11, *F–J*). In myenteric ganglion obtained from all experimental groups, double staining showed that OTX1 immunoreactivity was

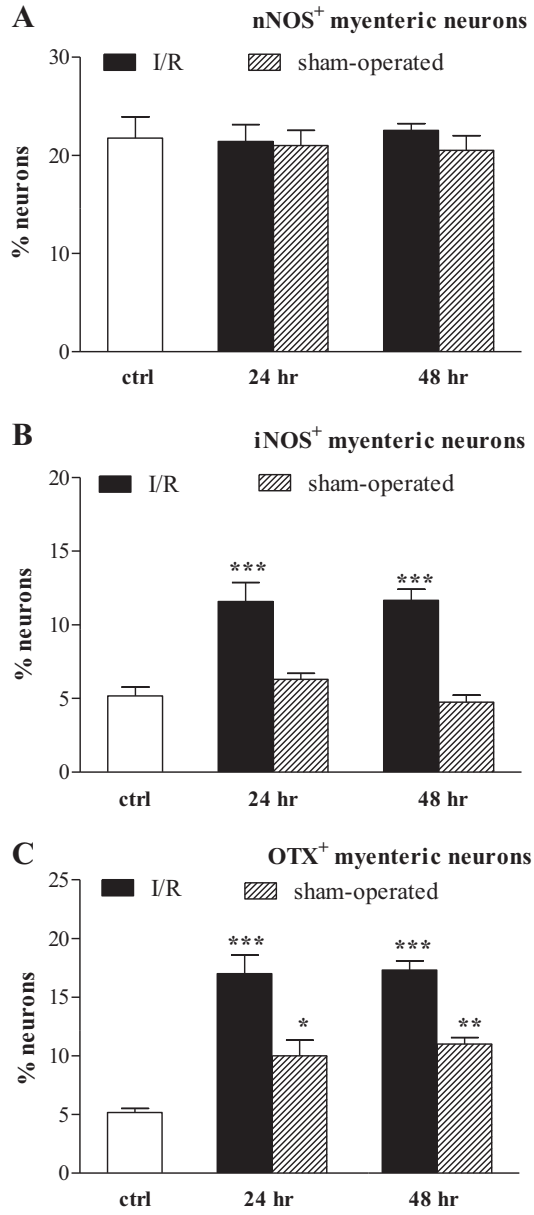

Fig. 9. Percentage of rat small intestine myenteric neurons staining for nNOS, iNOS, and pan-OTX antibodies in control conditions and during I/R. *A–C*: percentage of myenteric neurons per mm^2 staining for HUC/D and immunopositive for nNOS (*A*), iNOS (*B*), and OTX (*C*) in rat small intestine whole mounts preparations obtained from control animals (empty bars), at 24 and 48 h after inducing in vivo I/R (solid bars), and in the relative sham-operated animals (slashed bars). Values are expressed as means ± SE of 4 experiments. $*P < 0.05$, $**P < 0.01$, $***P < 0.001$ vs. control animals by one-way ANOVA followed by Tukey's test.

highly superimposable with iNOS labeling, whereas OTX1 immunostaining myenteric neurons were not positive to nNOS as shown in Fig. 12, *A–F*. In all experimental groups, almost all OTX2-immunoreactive neurons stained for nNOS (Fig. 12, *G–I*). There was no evidence of costaining between OTX2 and iNOS as shown in Fig. 12, *J–L*.

DISCUSSION

The present study strengthens the inference that after in vivo I/R damage to the intestine, both nNOS and iNOS expressing myenteric neurons may undergo important changes that sustain derangements of motor function (24, 54, 56). In these conditions, the number of iNOS-expressing neurons is increased, while nNOS-immunopositive neurons, which are fundamental

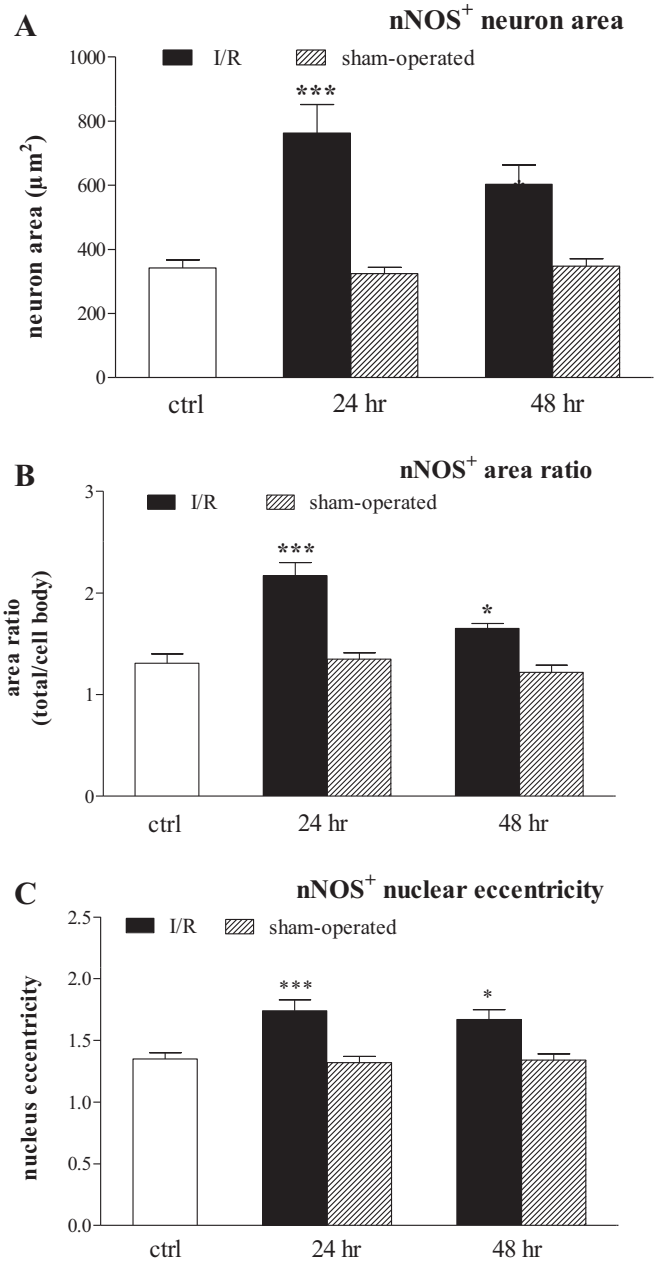

Fig. 10. Morphological analysis of nNOS immunoreactive neurons in rat small intestine whole mounts preparations after I/R. *A*: nNOS cell profile areas, including dendrites obtained from control animals (empty bars), at 24 and 48 h after inducing in vivo I/R (solid bars) and in the relative sham-operated animals (slashed bars). *B*: ratios of total cell areas, including dendrites, to cell body area (obtained from control animals (empty bars), at 24 and 48 h after inducing in vivo I/R (solid bars), and in the relative sham-operated animals (slashed bars). *C*: nuclear eccentricity (ratio of the major and minor diameters), obtained from control animals (empty bars), at 24 and 48 h after inducing in vivo I/R (solid bars), and in the relative sham-operated animals (slashed bars).Values are expressed as means ± SE of 4–6 experiments. $*P < 0.05$, $***P < 0.001$ vs. control animals by one way ANOVA followed by Tukey's test.

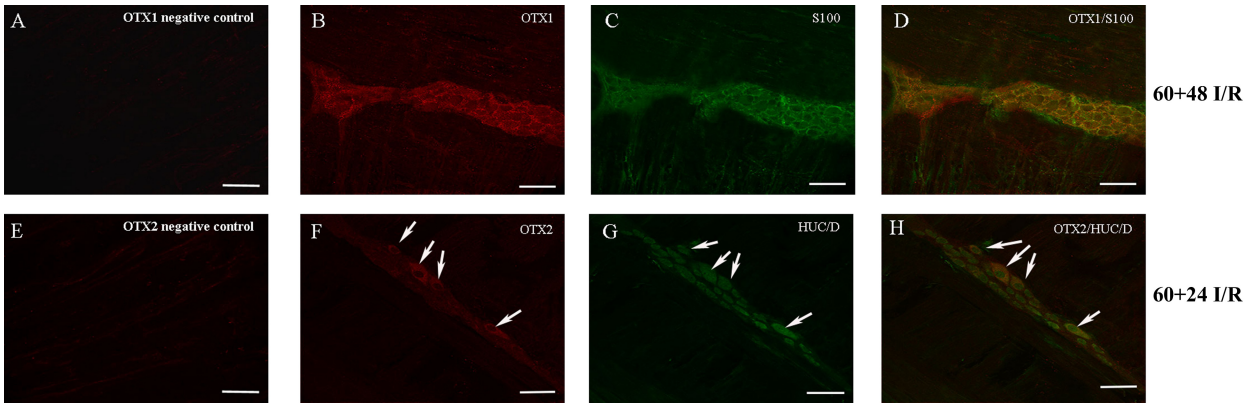

Fig. 11. Confocal images showing immunohistochemical localization of OTX1 and OTX2 in whole mount preparations of the rat small intestine obtained 24 and 48 h after inducing in vivo I/R. *A–D*: colocalization of OTX1 with the glial marker S100. *A*: OTX1 negative control obtained after incubation with nonimmune rabbit serum. *E–J*: colocalization of OTX2 with the neuronal marker HUC/D. *E*: OTX2 negative control obtained after incubation with nonimmune goat serum. Arrows indicate OTX2- and HUC/D-positive myenteric neurons (*F–J*). Bar = 50 μm.

for normal propulsion, are damaged, and both changes could contribute to I/R-mediated slowing of transit. In addition, to our knowledge, we provide the first morphological and biomolecular data suggesting that NO produced by iNOS and nNOS exerts a modulatory role on the expression of vital transcription factors orthodenticle homeobox protein 1 and 2 (OTX1 and OTX2) during I/R damage.

Yin and yang of iNOS and nNOS after I/R damage. In good agreement with rat, mice, and human data (9, 54, 64), in our model, re-establishment of blood flow after segmental mesenteric vascular occlusion induced a rapid infiltration of neutrophils in the external intestinal muscular layer secreting dangerous molecules, including myeloperoxidase (MPO). In particular, reperfusion of the rat small intestine after ischemia induced an increase in neutrophil infiltration in both the submucosal and smooth muscle layers, which reached statistical significance 24 h after the SMA occlusion. Accordingly, MPO activity increased during the reperfusion period in mucosa-deprived intestinal segments reaching a maximum after 24 h.

The significant reduction of small intestine transit after both 60 min of ischemia and after 48 h of reperfusion reflects the occurrence of adaptive changes in the intestinal motor function after the I/R damage. In particular, the slowing of transit observed after 60 min of ischemia may represent an acute response to energy depletion and hypoxic injury (67). Accordingly, in the mouse jejunum after 60 min of in vitro ischemia the frequency of spontaneous contractions were drastically reduced while the response to electrical transmural stimulation was completely abolished (10). Analogous observations were obtained in guinea pig ileum after an in vivo ischemic challenge (57).

In our study, restoration of normal metabolic conditions resulted in initial improvement in intestinal motility, but further reduction of transit was observed after 48 h of reperfusion. Subsequently, in agreement with other studies, the efficiency of the intestinal transit returned to control values by 72 h (8). The major changes observed 24 to 48 h after reperfusion for both neutrophil infiltration and intestinal transit suggest that these time periods may be crucial for the development of damages to the external muscular layer and the attached myenteric plexus, which is reflected by the histological data showing cellular suffering in both neurons and smooth muscle cells. Consistent with this notion, in longitudinal muscle myenteric plexus preparations (LMMPs), the amount of hypoxia-inducible factor-1α (HIF1α) mRNA significantly increased both at 24 and 48 h after I/R. HIF1α is a key regulator of the genomic response to hypoxia in both physiological and pathophysiological conditions since it may sustain the encoding of proteins involved in cellular energy preservation and that support tissue oxygenation, such as vascular endothelial growth factor-α (VEGFα) (15). Interestingly, target VEGFα transcript levels were also elevated at 24 and 48 h after I/R. In the sham-operated group at 24 h after neutrophil infiltration, HIF1α and VEGFα transcript levels were elevated, indicating likely inflammatory damage induced by laparatomy. Indeed, during active intestinal inflammation, such as IBD, these three parameters are upregulated (4, 7, 17, 25).

Focusing on the possible divergent roles of nNOS and iNOS in myenteric ganglia after an I/R, our immunohistochemical findings suggest that in the rat small intestine, as previously seen in guinea pig and mouse, the normal 22% nNOS containing myenteric neurons among the total myenteric neuron population, was unchanged (17, 54). Accordingly, protein and transcript levels of nNOS in LMMPs were also unchanged. However, the morphology of this subset of myenteric neurons was profoundly affected, with swollen cytoplasm, enlarged and distorted dendrites, and nuclear eccentricity. This supports the notion of selective damage to nNOS containing myenteric neurons after an I/R injury to the gut (55, 60). Also in accord with other reports, in control conditions a small number of rat small intestine myenteric neurons stain for iNOS, representing about 6% of the myenteric neurons (24, 27, 46). Notably, iNOS is also expressed in enteric glial cells, which represent an important nonneuronal component of the enteric nervous system and share many similarities with central nervous system astrocytes. Several studies have demonstrated that enteric glial cells, in analogy with the function of astrocytes, not only contribute to a protective local microenvironment but may also function in enteric information transfer via neuroligand action (28, 58). iNOS expressed by enteric glia may then participate in intestinal I/R damage, as does iNOS expressed by astrocytes after an ischemic injury to the brain (3).

The number of iNOS immunostaining myenteric neurons significantly increased at 24 and 48 h after I/R; and consistent

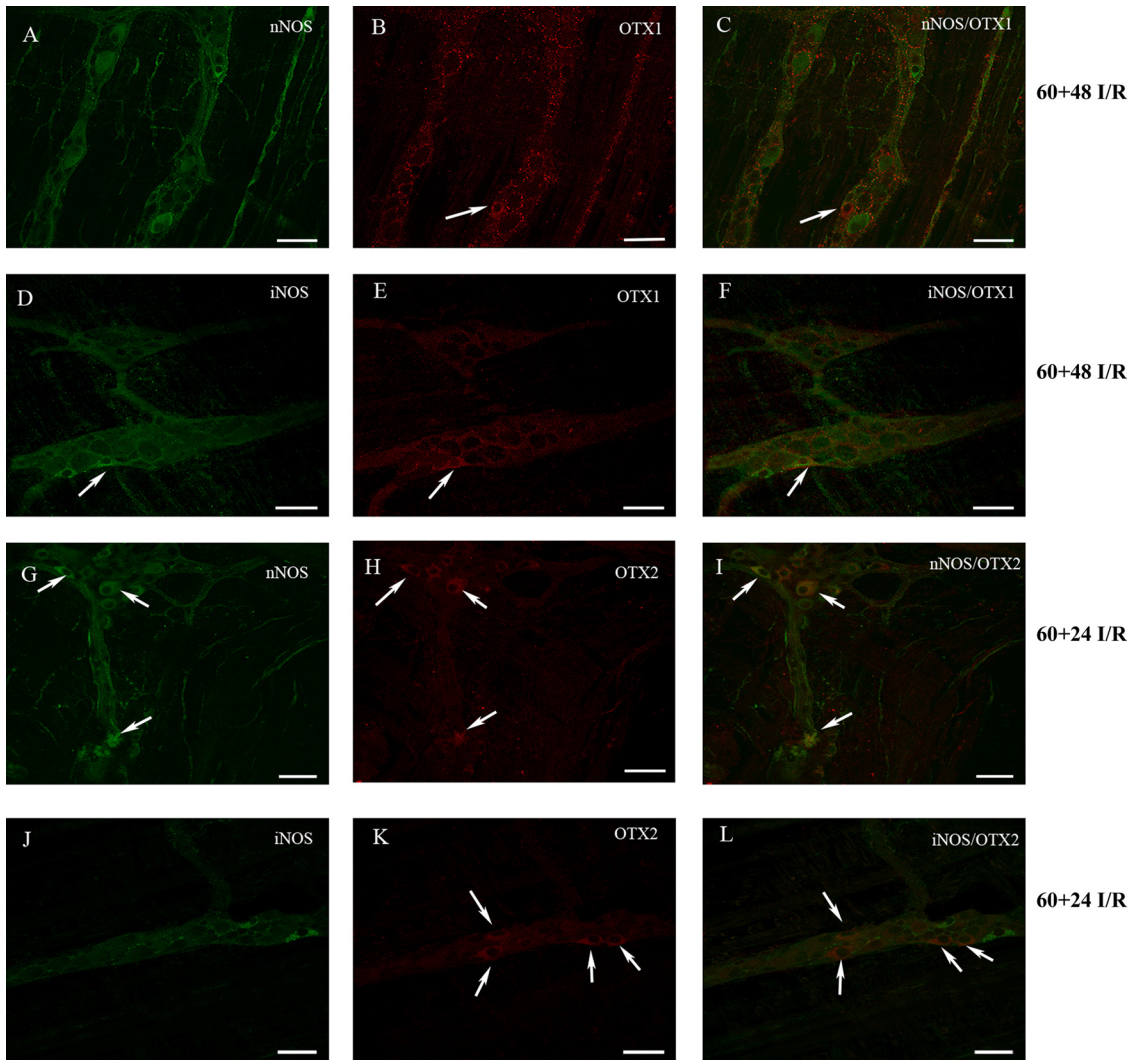

Fig. 12. Confocal images showing colocalization of OTX1 and OTX2 with nNOS and iNOS in whole mount preparations of the rat small intestine during I/R. *A–F*: colocalization of OTX1 with nNOS and iNOS in the small intestine of animals subjected to 60 min of in vivo ischemia followed by 48 h of reperfusion preparations. *G–L*: colocalization of OTX2 with nNOS and iNOS in whole mount preparations of the rat small intestine obtained from animals subjected to 60 min of in vivo ischemia followed by 24 h of reperfusion. arrows indicate myenteric neurons positive for OTX1 but not for nNOS (*B* and *C*) and neurons staining for OTX1 and iNOS (*D–F*). Arrows indicate myenteric neurons staining for OTX2 and nNOS (*G–I*) and neurons positive for OTX2 but not for iNOS (*K* and *L*). Bar = 50 μm.

with other reports for neuronal cells (47, 72), both transcript and protein levels of iNOS significantly increased. Interestingly, the results parallel those for HIF1α, a potent modulator of iNOS mRNA transcription under I/R conditions (35).

The ability of 1400W to modulate iNOS mRNA at 24 and 48 h after I/R suggests a possible autoregulation of NO levels. Both positive and negative feedback mechanisms for NO levels have been suggested (1). In our study, pretreatment with 1400W attenuated I/R-induced increase of iNOS protein levels more than iNOS mRNA levels, suggesting the occurrence of a positive feedback pathway which amplifies iNOS translation more than transcription.

The ability of 1400W and NPLA to reduce I/R-induced enhancement of MPO activity in intestinal whole wall specimens after 24 and 48 h of reperfusion suggests that both iNOS-and nNOS-derived NO may take part to neutrophil recruitment after an ischemic damage to the gut. In this view, as observed in other peripheral tissues, NO produced by nNOS not only represents a primary enteric neurotransmitter but may also participate to the development of intestinal I/R injury (16).

However, when considering the neuromuscular transmission, the ability of NPLA to reduce small intestinal transit in control and sham-operated animals strengthens the concept that intestinal motility strictly relies upon the integrity of nNOS function. In fact, at 48 h after I/R, greater transit slowing was seen after nNOS selective blockade, consistent with previous findings (8, 56). By contrast, at 48 h after I/R, iNOS blockade restored efficiency of intestinal transit to control values, consistent with overproduction of iNOS-derived NO as detrimental to intestinal motor function (9) Overall, nitrergic myenteric neurons may gain functional plasticity by balancing NOS isoforms (24, 61). nNOS may be the major source of NO in the physiological modulation of nonadrenergic noncholinergic motor responses, exerting a protective effect during I/R injury, while upregulation of iNOS in these conditions would rather enhance intestinal motor derangements.

Molecular mechanism of iNOS vs. nNOS action. The molecular mechanism/s underpinning the neurodamaging and neuroprotective actions of iNOS and nNOS on myenteric neurons during I/R injury have not been clearly elucidated. NO has been described to participate to the I/R injury by diverse molecular and biochemical pathways including activation of transcription factors (44). Here we show that in myenteric ganglia NO produced by either nNOS or iNOS after an I/R injury may influence the availability of two homeobox transcription factors, OTX1 and OTX2, both essential for brain development (48, 61). OTX1 and OTX2 expression in adult brain and soma is generally low, but several reports suggest that both transcription factors may participate in tumor growth or inflammatory injury (5, 14, 70). Ours is the first to assess the possible involvement of OTX1 and OTX2 in the response of myenteric ganglia to I/R injury. Both homeobox proteins are indeed expressed in the myenteric plexus of the rat small intestine: OTX1, predominantly in enteric glial cells, and OTX2, uniquely in neuronal cells. Importantly, we find both upregulated after I/R damage, with increased numbers of myenteric neurons positive for OTX. Interestingly, while OTX1 transcription was upregulated at 24 h and further elevated at 48 h of reperfusion, OTX2 transcript and protein were maximally elevated at 24 h of reperfusion and declined toward control values at 48 h. The observation that both OTX1 and OTX2 are expressed in normal adult rat myenteric ganglia and, all the more, that their levels of expression may change after I/R injury is highly suggestive that both proteins may have a role in the modulation of intestinal neuromuscular functions. Noteworthy, major changes in the number and function of both excitatory and inhibitory enteric neuronal pathways may occur in response to deletion of a homeobox gene phylogenetically related to OTX, Ncx/Hox11L.1, which retains a fundamental role for enteric ganglia development (2, 38, 48, 69).

Because sham-operated groups showed more OTX1 and OTX2 mRNA than control LMMPs, OTX1 and OTX2 may be sensitive to the inflammatory challenge associated with laparatomy. In this regard, several reports suggest that CDX2, an intestine-specific homeodomain transcription factor phylogenetically related to OTX, is involved in the development of inflammatory responses in the gut (13).

NPLA and 1400W were able to drastically reduce I/R-induced OTX1 and OTX2 mRNA and protein levels in LMMPs, suggesting that NO derived from both iNOS and nNOS regulates OTX1 and OTX2 transcription and translation in this model. However, 1400W modulates OTX1 mRNA and protein levels more efficiently, indicating a more consequential involvement of iNOS, as confirmed by the superimposition of OTX1 with iNOS staining, but not with nNOS, in rat small intestine myenteric plexus. By contrast, upregulation of OTX2 mRNA and protein was more sensitive to NPLA, indicating greater selectivity for nNOS, as confirmed by the superimposition of nNOS and OTX2 immunostaining in myenteric ganglia.

NO may thus modulate myenteric and glial function by promoting OTX1 and OTX2 upregulation, with NO derived from iNOS promoting OTX1 upregulation more, while nNOS seems to be more closely related to OTX2 upregulation. We hypothesize that the neurodamaging and neuroprotective roles of iNOS and nNOS during I/R injury in the gut may thus involve corresponding activation of molecular pathways downstream of OTX1 and OTX2, respectively. On the whole these observation are highly suggestive that an interplay between myenteric nitrergic pathways and OTX transcription factors may sustain NO-mediated development of altered motor responses after intestinal I/R injury. Interestingly, a preferential involvement of enteric nitrergic inhibitory pathways underlays development of dysmotility in Ncx/Hox11L.1$^{-/-}$ mice (38).

Intestinal ischemia is a rarely preventable event and most research in the field has focused on advancing techniques for early detection of ischemia and the development of novel therapeutic approaches that target the reperfusion period following the ischemic insult. One of the more promising approaches is to individuate molecular pathways underpinning cell damage and the superimposed inflammatory reaction, which on its own may exacerbate I/R injury and hampers tissue repair. Development of new therapeutic strategies in this field comprise the modulation of cell death pathways as well as the repair processes (26). In this perspective our data, by providing new hints on the possible sources for NO in the myenteric plexus after an I/R injury and by describing new molecular pathways linked to its production, may contribute to the development of novel strategies for the treatment of gastrointestinal diseases such as I/R injury.

ACKNOWLEDGMENTS

We thank Dr. Valeria Prandoni and Dr. Michela Bistoletti for the skilful assistance in performing some experiments. Dr. Fabrizio Bolognese is kindly acknowledged for the excellent assistance in the acquisition of confocal images.

GRANTS

This study was performed with grants from the Italian Ministry of University and Research (PRIN 2008) and the Universities of Insubria and of Pavia (FAR 2009–2014).

DISCLOSURES

No conflicts of interest, financial or otherwise, are declared by the author(s).

AUTHOR CONTRIBUTIONS

V.F., E.C., S.M., C.P., A.C., A.R., E.M., A.M.C., A.M., and C.G. performed experiments; V.F., E.C., S.M., C.P., A.C., A.R., E.M., A.M.C., and C.G. analyzed data; V.F., E.C., S.M., C.P., A.M.C., A.M., and C.G. interpreted results of experiments; V.F., E.C., S.M., and C.G. prepared figures; V.F., E.C., and C.G. drafted manuscript; V.F., E.C., S.M., C.P., A.C., A.R., E.M., A.M.C., I.Z., A.M., D.N., F.C., G.F., C.G., and G.P. approved final version of manuscript; I.Z., A.M., D.N., F.C., G.F., and G.P. edited and revised manuscript; C.G. and G.P. conceived and designed research.

REFERENCES

1. **Aktan F.** iNOS-mediated nitric oxide production and its regulation. *Life Sci* 75: 639–653, 2004. doi:10.1016/j.lfs.2003.10.042.
2. **Aoki T, Jusuf AA, Iitsuka Y, Isono K, Tokuhisa T, Hatano M.** Ncx (Enx, Hox11L.1) is required for neuronal cell death in enteric ganglia of mice. *J Pediatr Surg* 42: 1081–1088, 2007. doi:10.1016/j.jpedsurg.2007.01.064.
3. **Askalan R, Deveber G, Ho M, Ma J, Hawkins C.** Astrocytic-inducible nitric oxide synthase in the ischemic developing human brain. *Pediatr Res* 60: 687–692, 2006. doi:10.1203/01.pdr.0000246226.89215.a6.
4. **Aulí M, Nasser Y, Ho W, Burgueño JF, Keenan CM, Romero C, Sharkey KA, Fernández E.** Neuromuscular changes in a rat model of colitis. *Auton Neurosci* 141: 10–21, 2008. doi:10.1016/j.autneu.2008.04.005.
5. **Azzolini C, Pagani IS, Pirrone C, Borroni D, Donati S, Al Oum M, Pigni D, Chiaravalli AM, Vinciguerra R, Simonelli F, Porta G.** Expression of VEGF-A, Otx homeobox and p53 family genes in proliferative

vitreoretinopathy. *Mediators Inflamm* 2013: 857380, 2013. doi:10.1155/2013/857380.
6. **Bagyánszki M, Torfs P, Krecsmarik M, Fekete E, Adriaensen D, Van Nassauw L, Timmermans JP, Kroese AB.** Chronic alcohol consumption induces an overproduction of NO by nNOS- and iNOS-expressing myenteric neurons in the murine small intestine. *Neurogastroenterol Motil* 23: e237–e248, 2011. doi:10.1111/j.1365-2982.2011.01707.x.
7. **Bakirtzi K, West G, Fiocchi C, Law IK, Iliopoulos D, Pothoulakis C.** The neurotensin-HIF-1α-VEGFα axis orchestrates hypoxia, colonic inflammation, and intestinal angiogenesis. *Am J Pathol* 184: 3405–3414, 2014. doi:10.1016/j.ajpath.2014.08.015.
8. **Ballabeni V, Barocelli E, Bertoni S, Impicciatore M.** Alterations of intestinal motor responsiveness in a model of mild mesenteric ischemia/reperfusion in rats. *Life Sci* 71: 2025–2035, 2002. doi:10.1016/S0024-3205(02)01966-5.
9. **Barocelli E, Ballabeni V, Ghizzardi P, Cattaruzza F, Bertoni S, Lagrasta CA, Impicciatore M.** The selective inhibition of inducible nitric oxide synthase prevents intestinal ischemia-reperfusion injury in mice. *Nitric Oxide* 14: 212–218, 2006. doi:10.1016/j.niox.2005.11.006.
10. **Bielefeldt K, Conklin JL.** Intestinal motility during hypoxia and reoxygenation in vitro. *Dig Dis Sci* 42: 878–884, 1997. doi:10.1023/A:1018899927786.
11. **Bradley PP, Priebat DA, Christensen RD, Rothstein G.** Measurement of cutaneous inflammation: estimation of neutrophil content with an enzyme marker. *J Invest Dermatol* 78: 206–209, 1982. doi:10.1111/1523-1747.ep12506462.
12. **Bult H, Boeckxstaens GE, Pelckmans PA, Jordaens FH, Van Maercke YM, Herman AG.** Nitric oxide as an inhibitory non-adrenergic non-cholinergic neurotransmitter. *Nature* 345: 346–347, 1990. doi:10.1038/345346a0.
13. **Coskun M, Troelsen JT, Nielsen OH.** The role of CDX2 in intestinal homeostasis and inflammation. *Biochim Biophys Acta* 1812: 283–289, 2011. doi:10.1016/j.bbadis.2010.11.008.
14. **Di C, Liao S, Adamson DC, Parrett TJ, Broderick DK, Shi Q, Lengauer C, Cummins JM, Velculescu VE, Fults DW, McLendon RE, Bigner DD, Yan H.** Identification of OTX2 as a medulloblastoma oncogene whose product can be targeted by all-trans retinoic acid. *Cancer Res* 65: 919–924, 2005.
15. **Dirnagl U, Becker K, Meisel A.** Preconditioning and tolerance against cerebral ischaemia: from experimental strategies to clinical use. *Lancet Neurol* 8: 398–412, 2009. doi:10.1016/S1474-4422(09)70054-7.
16. **Duma D, Fernandes D, Bonini MG, Stadler K, Mason RP, Assreuy J.** NOS-1-derived NO is an essential triggering signal for the development of systemic inflammatory responses. *Eur J Pharmacol* 668: 285–292, 2011. doi:10.1016/j.ejphar.2011.05.065.
17. **Feinman R, Deitch EA, Watkins AC, Abungu B, Colorado I, Kannan KB, Sheth SU, Caputo FJ, Lu Q, Ramanathan M, Attan S, Badami CD, Doucet D, Barlos D, Bosch-Marce M, Semenza GL, Xu DZ.** HIF-1 mediates pathogenic inflammatory responses to intestinal ischemia-reperfusion injury. *Am J Physiol Gastrointest Liver Physiol* 299: G833–G843, 2010. doi:10.1152/ajpgi.00065.2010.
18. **Ferrer-Sueta G, Radi R.** Chemical biology of peroxynitrite: kinetics, diffusion, and radicals. *ACS Chem Biol* 4: 161–177, 2009. doi:10.1021/cb800279q.
19. **Filpa V, Carpanese E, Marchet S, Prandoni V, Moro E, Lecchini S, Frigo G, Giaroni C, Crema F.** Interaction between NMDA glutamatergic and nitrergic enteric pathways during in vitro ischemia and reperfusion. *Eur J Pharmacol* 750: 123–131, 2015. doi:10.1016/j.ejphar.2015.01.021.
20. **Gariepy CE.** Intestinal motility disorders and development of the enteric nervous system. *Pediatr Res* 49: 605–613, 2001. doi:10.1203/00006450-200105000-00001.
21. **Garvey EP, Oplinger JA, Furfine ES, Kiff RJ, Laszlo F, Whittle BJ, Knowles RG.** 1400W is a slow, tight binding, and highly selective inhibitor of inducible nitric-oxide synthase in vitro and in vivo. *J Biol Chem* 272: 4959–4963, 1997. doi:10.1074/jbc.272.8.4959.
22. **Giaroni C, Zanetti E, Pascale A, Oldrini R, Canciani L, Giuliani D, Amadio M, Chiaravalli AM, Lecchini S, Frigo GM.** Involvement of Ca^{2+}-dependent PKCs in the adaptive changes of mu-opioid pathways to sympathetic denervation in the guinea pig colon. *Biochem Pharmacol* 78: 1233–1241, 2009. doi:10.1016/j.bcp.2009.06.107.
23. **Giaroni C, Zanetti E, Giuliani D, Oldrini R, Marchet S, Moro E, Borroni P, Trinchera M, Crema F, Lecchini S, Frigo G.** Protein kinase C modulates NMDA receptors in the myenteric plexus of the guinea pig ileum during in vitro ischemia and reperfusion. *Neurogastroenterol Motil* 23: e91–e103, 2011. doi:10.1111/j.1365-2982.2010.01644.x.
24. **Giaroni C, Marchet S, Carpanese E, Prandoni V, Oldrini R, Bartolini B, Moro E, Vigetti D, Crema F, Lecchini S, Frigo G.** Role of neuronal and inducible nitric oxide synthases in the guinea pig ileum myenteric plexus during in vitro ischemia and reperfusion. *Neurogastroenterol Motil* 25: e114–e126, 2013. doi:10.1111/nmo.12061.
25. **Giatromanolaki A, Sivridis E, Maltezos E, Papazoglou D, Simopoulos C, Gatter KC, Harris AL, Koukourakis MI.** Hypoxia inducible factor 1α and 2α overexpression in inflammatory bowel disease. *J Clin Pathol* 56: 209–213, 2003. doi:10.1136/jcp.56.3.209.
26. **Gonzalez LM, Moeser AJ, Blikslager AT.** Animal models of ischemia-reperfusion-induced intestinal injury: progress and promise for translational research. *Am J Physiol Gastrointest Liver Physiol* 308: G63–G75, 2015. doi:10.1152/ajpgi.00112.2013.
27. **Green CL, Ho W, Sharkey KA, McKay DM.** Dextran sodium sulfate-induced colitis reveals nicotinic modulation of ion transport via iNOS-derived NO. *Am J Physiol Gastrointest Liver Physiol* 287: G706–G714, 2004. doi:10.1152/ajpgi.00076.2004.
28. **Gulbransen BD, Sharkey KA.** Novel functional roles for enteric glia in the gastrointestinal tract. *Nat Rev Gastroenterol Hepatol* 9: 625–632, 2012. doi:10.1038/nrgastro.2012.138.
29. **Haglund U, Bergqvist D.** Intestinal ischemia–the basics. *Langenbecks Arch Surg* 384: 233–238, 1999. doi:10.1007/s004230050197.
30. **Hassoun HT, Weisbrodt NW, Mercer DW, Kozar RA, Moody FG, Moore FA.** Inducible nitric oxide synthase mediates gut ischemia/reperfusion-induced ileus only after severe insults. *J Surg Res* 97: 150–154, 2001. doi:10.1006/jsre.2001.6140.
31. **Housset M, Samuel A, Ettaiche M, Bemelmans A, Béby F, Billon N, Lamonerie T.** Loss of Otx2 in the adult retina disrupts retinal pigment epithelium function, causing photoreceptor degeneration. *J Neurosci* 33: 9890–9904, 2013. doi:10.1523/JNEUROSCI.1099-13.2013.
32. **Hsu SM, Raine L.** Protein A, avidin, and biotin in immunohistochemistry. *J Histochem Cytochem* 29: 1349–1353, 1981. doi:10.1177/29.11.6172466.
33. **Kalogeris T, Baines CP, Krenz M, Korthuis RJ.** Cell biology of ischemia/reperfusion injury. *Int Rev Cell Mol Biol* 298: 229–317, 2012. doi:10.1016/B978-0-12-394309-5.00006-7.
34. **Kankuri E, Vaali K, Knowles RG, Lähde M, Korpela R, Vapaatalo H, Moilanen E.** Suppression of acute experimental colitis by a highly selective inducible nitric-oxide synthase inhibitor, N-[3-(aminomethyl) benzyl]acetamidine. *J Pharmacol Exp Ther* 298: 1128–1132, 2001.
35. **Kannan KB, Colorado I, Reino D, Palange D, Lu Q, Qin X, Abungu B, Watkins A, Caputo FJ, Xu DZ, Semenza GL, Deitch EA, Feinman R.** Hypoxia-inducible factor plays a gut-injurious role in intestinal ischemia reperfusion injury. *Am J Physiol Gastrointest Liver Physiol* 300: G853–G861, 2011. doi:10.1152/ajpgi.00459.2010.
36. **Kapur RP, Gershon MD, Milla PJ, Pachnis V.** The influence of Hox genes and three intercellular signalling pathways on enteric neuromuscular development. *Neurogastroenterol Motil* 16, *Suppl* 1: 8–13, 2004. doi:10.1111/j.1743-3150.2004.00467.x.
37. **Kato S, Kawahara R, Yasuda M, Amagase K, Takeuchi K.** Aggravation of cold-restraint stress-induced gastric lesions in adjuvant arthritic rats: pathogenic role of inducible and endothelial nitric oxide. *J Pharmacol Sci* 111: 244–252, 2009. doi:10.1254/jphs.09203FP.
38. **Kobayashi H, Kusafuka J, Lane GJ, Yamataka A, Satoh K, Hayakawa T, Kase Y, Hatano M.** The mechanism of intestinal motility in homozygous mutant Ncx/Hox11L.1-deficient mice–a model for intestinal neuronal dysplasia. *J Pediatr Surg* 42: 2062–2066, 2007. doi:10.1016/j.jpedsurg.2007.08.029.
39. **Laemmli UK.** Cleavage of structural proteins during the assembly of the head of bacteriophage T4. *Nature* 227: 680–685, 1970. doi:10.1038/227680a0.
40. **Limb GA, Salt TE, Munro PM, Moss SE, Khaw PT.** In vitro characterization of a spontaneously immortalized human Müller cell line (MIO-M1). *Invest Ophthalmol Vis Sci* 43: 864–869, 2002.
41. **Lindeström LM, Ekblad E.** Structural and neuronal changes in rat ileum after ischemia with reperfusion. *Dig Dis Sci* 49: 1212–1222, 2004. doi:10.1023/B:DDAS.0000037815.63547.08.
42. **Lisowski P, Juszczak GR, Goscik J, Stankiewicz AM, Wieczorek M, Zwierzchowski L, Swiergiel AH.** Stress susceptibility-specific phenotype associated with different hippocampal transcriptomic responses to chronic tricyclic antidepressant treatment in mice. *BMC Neurosci* 14: 144, 2013. doi:10.1186/1471-2202-14-144.

43. **Livak KJ, Schmittgen TD.** Analysis of relative gene expression data using real-time quantitative PCR and the 2(-delta delta C(T)) method. *Methods* 25: 402–408, 2001. doi:10.1006/meth.2001.1262.
44. **Mallick IH, Yang W, Winslet MC, Seifalian AM.** Ischemia-reperfusion injury of the intestine and protective strategies against injury. *Dig Dis Sci* 49: 1359–1377, 2004. doi:10.1023/B:DDAS.0000042232.98927.91.
45. **Matthijsen RA, Derikx JPM, Kuipers D, van Dam RM, Dejong CH, Buurman WA.** Enterocyte shedding and epithelial lining repair following ischemia of the human small intestine attenuate inflammation. *PLoS One* 4: e7045, 2009. doi:10.1371/journal.pone.0007045.
46. **Miampamba M, Sharkey KA.** Temporal distribution of neuronal and inducible nitric oxide synthase and nitrotyrosine during colitis in rats. *Neurogastroenterol Motil* 11: 193–206, 1999. doi:10.1046/j.1365-2982.1999.00150.x.
47. **Moro MA, De Alba J, Leza JC, Lorenzo P, Fernández AP, Bentura ML, Boscá L, Rodrigo J, Lizasoain I.** Neuronal expression of inducible nitric oxide synthase after oxygen and glucose deprivation in rat forebrain slices. *Eur J Neurosci* 10: 445–456, 1998. doi:10.1046/j.1460-9568.1998.00028.x.
48. **Nam J, Nei M.** Evolutionary change of the numbers of homeobox genes in bilateral animals. *Mol Biol Evol* 22: 2386–2394, 2005. doi:10.1093/molbev/msi229.
49. **Palombo R, Porta G, Bruno E, Provero P, Serra V, Neduri K, Viziano A, Alessandrini M, Micarelli A, Ottaviani F, Melino G, Terrinoni A.** OTX2 regulates the expression of TAp63 leading to macular and cochlear neuroepithelium development. *Aging (Albany NY)* 7: 928–936, 2015. doi:10.18632/aging.100839.
50. **Pontell L, Sharma P, Rivera LR, Thacker M, Tan YH, Brock JA, Furness JB.** Damaging effects of ischemia/reperfusion on intestinal muscle. *Cell Tissue Res* 343: 411–419, 2011. doi:10.1007/s00441-010-1096-z.
51. **Prochiantz A, Fuchs J, Di Nardo AA.** Postnatal signalling with homeoprotein transcription factors. *Philos Trans R Soc Lond B Biol Sci* 369: 20130518, 2014. doi:10.1098/rstb.2013.0518.
52. **Puig MM, Warner W, Pol O.** Intestinal inflammation and morphine tolerance alter the interaction between morphine and clonidine on gastrointestinal transit in mice. *Anesthesiology* 93: 219–230, 2000. doi:10.1097/00000542-200007000-00033.
53. **Reinus JF, Brandt LJ, Boley SJ.** Ischemic diseases of the bowel. *Gastroenterol Clin North Am* 19: 319–343, 1990.
54. **Rivera LR, Thacker M, Castelucci P, Bron R, Furness JB.** The reactions of specific neuron types to intestinal ischemia in the guinea pig enteric nervous system. *Acta Neuropathol* 118: 261–270, 2009. doi:10.1007/s00401-009-0549-5.
55. **Rivera LR, Poole DP, Thacker M, Furness JB.** The involvement of nitric oxide synthase neurons in enteric neuropathies. *Neurogastroenterol Motil* 23: 980–988, 2011. doi:10.1111/j.1365-2982.2011.01780.x.
56. **Rivera LR, Pontell L, Cho HJ, Castelucci P, Thacker M, Poole DP, Frugier T, Furness JB.** Knock out of neuronal nitric oxide synthase exacerbates intestinal ischemia/reperfusion injury in mice. *Cell Tissue Res* 349: 565–576, 2012. doi:10.1007/s00441-012-1451-3.
57. **Rodriguez R, Ventura-Martinez R, Santiago-Mejia J, Avila-Costa MR, Fortoul TI.** Altered responsiveness of the guinea-pig isolated ileum to smooth muscle stimulants and to electrical stimulation after in situ ischemia. *Br J Pharmacol* 147: 371–378, 2006. doi:10.1038/sj.bjp.0706618.
58. **Sarosi GA, Barnhart DC, Turner DJ, Mulholland MW.** Capacitative Ca^{2+} entry in enteric glia induced by thapsigargin and extracellular ATP. *Am J Physiol Gastrointest Physiol* 275: G550–G555, 1998.
59. **Schneider CA, Rasband WS, Eliceiri KW.** NIH Image to ImageJ: 25 years of image analysis. *Nat Methods* 9: 671–675, 2012. doi:10.1038/nmeth.2089.
60. **Silva MA, de Meirelles LR, Bustorff-Silva JM.** Changes in intestinal motility and in the myenteric plexus in a rat model of intestinal ischemia-reperfusion. *J Pediatr Surg* 42: 1062–1065, 2007. doi:10.1016/j.jpedsurg.2005.07.009.
61. **Spatazza J, Di Lullo E, Joliot A, Dupont E, Moya KL, Prochiantz A.** Homeoprotein signaling in development, health, and disease: a shaking of dogmas offers challenges and promises from bench to bed. *Pharmacol Rev* 65: 90–104, 2013. doi:10.1124/pr.112.006577.
62. **Talapka P, Bódi N, Battonyai I, Fekete E, Bagyánszki M.** Subcellular distribution of nitric oxide synthase isoforms in the rat duodenum. *World J Gastroenterol* 17: 1026–1029, 2011. doi:10.3748/wjg.v17.i8.1026.
63. **Thacker M, Rivera LR, Cho HJ, Furness JB.** The relationship between glial distortion and neuronal changes following intestinal ischemia and reperfusion. *Neurogastroenterol Motil* 23: e500–e509, 2011. doi:10.1111/j.1365-2982.2011.01696.x.
64. **Türler A, Kalff JC, Heeckt P, Abu-Elmagd KM, Schraut WH, Bond GJ, Moore BA, Brünagel G, Bauer AJ.** Molecular and functional observations on the donor intestinal muscularis during human small bowel transplantation. *Gastroenterology* 122: 1886–1897, 2002. doi:10.1053/gast.2002.33628.
65. **Van Noorden S, Stuart MC, Cheung A, Adams EF, Polak JM.** Localization of human pituitary hormones by multiple immunoenzyme staining procedures using monoclonal and polyclonal antibodies. *J Histochem Cytochem* 34: 287–292, 1986. doi:10.1177/34.3.2419389.
66. **Vannucchi MG, Corsani L, Bani D, Faussone-Pellegrini MS.** Myenteric neurons and interstitial cells of Cajal of mouse colon express several nitric oxide synthase isoforms. *Neurosci Lett* 326: 191–195, 2002. doi:10.1016/S0304-3940(02)00338-5.
67. **Walus KM, Jacobson ED.** Relation between small intestinal motility and circulation. *Am J Physiol Gastrointest Liver Physiol* 241: G1–G15, 1981.
68. **Wu R, Dong W, Wang Z, Jacob A, Cui T, Wang P.** Enhancing apoptotic cell clearance mitigates bacterial translocation and promotes tissue repair after gut ischemia-reperfusion injury. *Int J Mol Med* 30: 593–598, 2012. doi:10.3892/ijmm.2012.
69. **Yanai T, Kobayashi H, Yamataka A, Lane GJ, Miyano T, Hayakawa T, Satoh K, Kase Y, Hatano M.** Acetylcholine-related bowel dysmotility in homozygous mutant NCX/HOX11L.1-deficient (NCX-/-) mice-evidence that acetylcholine is implicated in causing intestinal neuronal dysplasia. *J Pediatr Surg* 39: 927–930, 2004. doi:10.1016/j.jpedsurg.2004.02.004.
70. **Yu K, Cai XY, Li Q, Yang ZB, Xiong W, Shen T, Wang WY, Li YF.** OTX1 promotes colorectal cancer progression through epithelial-mesenchymal transition. *Biochem Biophys Res Commun* 444: 1–5, 2014. doi:10.1016/j.bbrc.2013.12.125.
71. **Zhang HQ, Fast W, Marletta MA, Martasek P, Silverman RB.** Potent and selective inhibition of neuronal nitric oxide synthase by N omega-propyl-L-arginine. *J Med Chem* 40: 3869–3870, 1997. doi:10.1021/jm970550g.
72. **Zheng L, Ding J, Wang J, Zhou C, Zhang W.** Effects and mechanism of action of inducible nitric oxide synthase on apoptosis in a rat model of cerebral ischemia-reperfusion injury. *Anat Rec (Hoboken)* 299: 246–255, 2016. doi:10.1002/ar.23295.